

WRRI-UNC-89-246

MODELING ORGANIC CONTAMINANT SORPTION
IMPACTS ON AQUIFER RESTORATION

By

Cass T. Miller
Assistant Professor

Joseph A. Pedit
Research Assistant

Edward G. Staes
Research Assistant

Robert H. Gilbertsen
Research Assistant

Department of Environmental Sciences and Engineering
The University of North Carolina
Chapel Hill, North Carolina 27599

The research upon which this publication is based was supported by funds provided by the Water Resources Research Institute of The University of North Carolina.

WRRI Project No. 70078

July 1989

ACKNOWLEDGMENTS

This work was performed within the Department of Environmental Sciences and Engineering of the School of Public Health at the University of North Carolina at Chapel Hill. We wish to thank Dr. Aziz Amoozegar-Fard, from the Soil Science Department of North Carolina State University, for his cooperation and assistance on the sampling aspects of this project. We were fortunate in receiving first-class treatment and excellent cooperation from Marine Corps Base Camp Lejeune—specifically Mr. Robert E. Alexander and Colonel T. J. Dalzell. The Base contractors deserve thanks for their cooperation as well: Bert Lea and James Gonzales of Specialized Marine, Inc.; and Richard Catlin of Richard Catlin & Associates. We are indebted as well to the staff of the Department of Natural Resources and Community Development—Perry Nelson, Douglas Dixon, Charles Wakild, and Rick Shiver to name but a few—for their assistance in site location, needs assessment, and the monitoring well permitting aspects of the project.

ABSTRACT

The groundwater resources of the U.S. have been contaminated by a variety of organic pollutants that include solvents, petroleum products, and pesticides. A need exists to understand the movement of contaminants in the subsurface so that: (1) an assessment of the risk due to contamination may be made, (2) an economical and environmentally acceptable response to contamination may be designed, and (3) an appropriate ranking of sites that require clean-up and that are competing for the same fixed pool of resources may be accomplished. Many common organic contaminants sorb to solid surfaces, like soils or aquifer materials. Sorption affects the rate of transport for a given contaminant in the subsurface and may also affect the rate of contaminant degradation. An understanding of the sorption process is, therefore, an important part of understanding the overall movement of a contaminant in the subsurface.

This work focuses on the investigation of the sorption process in the subsurface. Specifically four aspects are considered: the measurement of sorption equilibrium for petroleum-based contaminants to a coastal North Carolina aquifer material; determination of the rate of sorption for these systems; development of mathematical models that may be used to simulate the sorption process; and an analysis of the significance of sorption-desorption rates for predicting field-scale transport of organic contaminants. Laboratory results demonstrate the relative importance of sorption as a function of compound type using aquifer material collected from a Camp Lejeune field site. The sorption process is shown to require several days to approach equilibrium, while the final equilibrium is found to be nonlinear. The analysis of sorption effects on time required for aquifer remediation shows that nonlinear desorption has a significant effect on remediation time, while the rate of desorption is shown to be less important for solute-solid combinations that sorb at a rate similar to those investigated in this work.

DISCLAIMER STATEMENT

Contents of this publication do not necessarily reflect the views and policies of the Water Resources Research Institute nor does mention of trade names or commercial products constitute their endorsement or recommendation for use by the Institute or the State of North Carolina.

TABLE OF CONTENTS

	<u>Page</u>
ACKNOWLEDGMENTS	ii
ABSTRACT	iii
LIST OF FIGURES	vii
LIST OF TABLES	ix
SUMMARY AND CONCLUSIONS	x
RECOMMENDATIONS	xii
INTRODUCTION	1
PREVIOUS RESEARCH	3
MATERIALS AND METHODS	7
MATERIALS	7
SOLUTE EXTRACTION AND MEASUREMENT METHODS	8
BOTTLE-POINT EXPERIMENTAL METHODS	11
COLUMN-REACTOR EXPERIMENTAL METHODS	12
MATHEMATICAL MODELING	15
GENERAL	15
SORPTION EQUILIBRIUM MODELS	15
SORPTION RATE SUB-MODELS	18
Batch-Reactor Model	18
Two-Site Model	18
Dual-Resistance Model	21
ADVECTIVE-DISPERSIVE-REACTIVE EQUATION MODELING	25
General Advective-Dispersive-Reactive Equation	25
One-Dimensional Local-Equilibrium Model	26
One-Dimensional Two-Site Model	28
One-Dimensional Dual-Resistance Model	30
RESULTS	33
BOTTLE-POINT EQUILIBRIUM EXPERIMENTAL RESULTS	33
BOTTLE-POINT RATE EXPERIMENTAL RESULTS	36
COLUMN-REACTOR EXPERIMENTAL RESULTS	41

	<u>Page</u>
DISCUSSION	47
GENERAL	47
CONSTITUTIVE APPROXIMATIONS OF SORPTION EQUILIBRIUM	48
EFFECT OF HYDRODYNAMICS ON AQUIFER REMEDIATION	50
EFFECT OF SORPTION EQUILIBRIUM ON AQUIFER REMEDIATION	54
EFFECT OF SORPTION RATE ON AQUIFER REMEDIATION	60
NOTATION	69
REFERENCES	73
APPENDIX I. FINITE ELEMENT DERIVATION FOR DUAL-RESISTANCE BATCH MODEL	79
APPENDIX II. FINITE DIFFERENCE DERIVATION FOR ONE-DIMENSIONAL TWO-SITE MODEL	83
APPENDIX III. FINITE DIFFERENCE DERIVATION FOR ONE-DIMENSIONAL DUAL-RESISTANCE MODEL	87

LIST OF FIGURES

1. Grain-size distribution for Camp Lejeune subsurface material.	9
2. Column-reactor system.	13
3. Dual-resistance model.	23
4. Sorption equilibrium data and model fits for the solute p-dichlorobenzene and the Camp Lejeune subsurface solid material.	34
5. Sorption equilibrium data and model fits for the solute o-xylene and the Camp Lejeune subsurface solid material.	35
6. Batch reactor sorption-rate data for the Camp Lejeune subsurface solid material.	38
7. Batch-reactor rate model fits to experimental data for the solute p-dichlorobenzene and the Camp Lejeune subsurface solid material.	40
8. Column tracer data and nonreactive advective-dispersive model fit.	42
9. Column data for organic solutes.	44
10. Column data for o-xylene and model predictions.	46
11. Dimensionless concentration profiles for linear, local-equilibrium sorption as a function of P_e	53
12. The effect of n_f on solute elution time for a step source of duration $\bar{t} = 3$	57
13. The effect of n_f on solute elution time for concentrations significantly less than the maximum system concentration.	58
14. The effect of n_f on solute elution time required to reach low concentration action levels.	59
15. Normalized concentration profiles as a function of D_a for $R_f = 2.0$ and $n_f = 1.0$	61
16. Normalized concentration profiles as a function of D_a for $R_f = 20.0$ and $n_f = 1.0$	62
17. Normalized concentration profiles as a function of D_a for $R_f = 2.0$ and $n_f = 0.8$	63
18. Normalized concentration profiles as a function of D_a for $R_f = 20.0$ and $n_f = 0.8$	64

19. The effect of D_a on solute elution time required to reach low concentration action levels for $R_f = 2.0$	66
20. The effect of D_a on solute elution time required to reach low concentration action levels for $R_f = 20.0$	67

LIST OF TABLES

1. Solid Material Characteristics.	8
2. Solute Properties.	10
3. Sorption Equilibrium Parameter Summary.	36
4. Sorption Rate Study Conditions and Parameter Summary.	37
5. Column Simulation Parameter Summary for o-Xylene.	45
6. Observed and Predicted Linear Partition Coefficients.	50

SUMMARY AND CONCLUSIONS

This research investigated the role of sorption-desorption phenomena on the aquifer restoration process. This research included three components: performance of laboratory experiments to observe the rate and equilibrium of sorption of moderately-hydrophobic organic solutes to aquifer sands; the derivation of mathematical models to describe laboratory sorption experiments; and the extension of mathematical models to investigate the significance of sorption-desorption rates on the rate of aquifer rehabilitation.

The laboratory experimental phase of this project investigated the rate and equilibrium of sorption of three moderately hydrophobic organic contaminants (toluene, o-xylene, and 1,4-dichlorobenzene) to aquifer material from a Camp Lejeune field site. The aquifer material was collected from the field site during the construction of a series of monitoring wells that are presently being used on a subsequent research project, which is sponsored by the U.S. Environmental Protection Agency. The results of the laboratory investigation show that for the coastal aquifer material studied: the fraction of organic carbon is very small ($f_{oc} = 2.4 \times 10^{-4}$); relatively little sorption occurs for simple aromatic compounds; and substantial amounts of sorption to the mineral surfaces of the subsurface material were not found—based on a reasonable agreement between organic-carbon-based correlations of predicted partitioning and measured values.

The models developed to simulate the laboratory data collected during this work include sorption equilibrium and sorption rate models. Sorption models were developed to simulate conditions in both completely-mixed batch reactors and in column reactors. Two conceptual models are presented: a two-site model and a dual-resistance model. The two-site model approximates the sorption process by assuming that a portion of sites in the aquifer solid phase sorb solute at a rapid rate and a portion of the sites in the solid phase sorb solute at a rate that may be approximated by a first-order expression. The dual-resistance model simulates the sorption process as function of two mass-transfer

resistances: diffusion through a stagnant boundary layer, and diffusion within a spherical solid particle.

The resultant mathematical models were solved using the finite-element method or the finite-difference method to approximate spatial derivatives and the Gear algorithm to resolve the temporally-dependent set of ordinary differential equations. Validation of the models shows the approximations to be accurate. The mathematical models, which were derived, were capable of simulating the laboratory data collected, with generally accurate results obtained.

Analysis of aquifer restoration shows that long remediation times can be due to several factors: subsurface heterogeneity, nonlinear desorption equilibrium, and sorption rate effects. Heterogeneity is hypothesized to be an important physical factor that contributes to long cleanup times. Nonlinear and hysteretic desorption equilibrium is shown to have a profound effect on aquifer remediation times—especially when remediation target-level concentrations are much smaller than the initial resident concentration. Sorption/desorption rate effects are shown to be a function of a dimensionless Damkohler number. Dimensionless analysis shows that sorption rate effects are a function of system scale (hydraulic retention time of the system). For sorption that occurs at a rate similar to the systems investigated in this work, sorption rate effects are expected to play a secondary role in contributing to prolonged aquifer remediation times.

RECOMMENDATIONS

The work summarized in this document suggests several recommendations; some that are immediately applicable, and some that require additional research. These recommendations may be summarized by:

1. Organic carbon analysis should be used routinely to provide a first-cut analysis of the relative importance of the sorption-desorption process.
2. The molecular topology method of Sabljic (1987) is an accurate constitutive method for predicting the extent of sorption in the subsurface.
3. Accurate predictions of aquifer cleanup times require knowledge of subsurface heterogeneity.
4. Nonlinear desorption equilibrium should be quantified and the effects included in the analysis of the time required for aquifer remediation.
5. The models developed in this report may be used to help estimate the clean-up time for a groundwater system.
6. Additional research is needed in several areas: the effect of subsurface heterogeneity on aquifer remediation times; the nature of desorption hysteresis; and the long-term nature of aquifer response to elution methods in the presence of a nonlinear sorbing organic solute.

INTRODUCTION

Millions of Americans depend on groundwater as a source of drinking water. Unfortunately, the valuable groundwater resources of the U.S. have been contaminated by pollutants originating from a variety of sources: leaking underground storage tanks and pipelines, toxic waste disposal areas, industrial spill areas, landfills, and lagoons.

Although a variety of cleanup options is available, the most widely used option is the purge-well method (Canter and Knox, 1986). The concept of purge wells is simple. One or more withdrawal wells is placed in the contaminated region of an aquifer. As pumping progresses over a period of time, the flow of water carries away the contaminated water. The solid material in the aquifer poses a special problem because some contaminants "sorb" to the solid phase. This contaminated solid phase can continue to cause problems by releasing sorbed contaminants long after wells remove the the original contaminated water. The single biggest cost of groundwater cleanup is often the energy cost of maintaining the pumping for the years required to cleanse an aquifer (Canter and Knox, 1986).

Given the high cost of cleaning contaminated aquifers in general, and given the high energy cost of purge-well systems in particular, accurate prediction of contaminant movement is crucial. Only by accurately understanding the movement of a groundwater contaminant plume can a groundwater professional provide a satisfactory measure to remedy the problem. In the case of purge wells in particular, accurate forecasts of cleanup time are vital to economical design.

One drawback of purge-well rehabilitation is the tailing phenomenon that has been observed for most cases concerning organic solute transport (e.g. Roberts et al., 1982). In the field and even in the lab researchers find that breakthrough response extends for considerably longer than expected. It appears that the contaminant sorbed to the solid phase takes longer to release than conventional models predict. Clearly, a field scale purge-well design based on a forecast that didn't include mechanisms that allow for a prediction of

the degree of tailing, could lead to grossly unrealistic conclusions concerning operation and maintenance costs. Since cleanup costs are typically large, this imprecision is important to examine.

The objectives of this research were to investigate the role of sorption equilibrium, and rate effects in contributing to contaminant tailing during aquifer rehabilitation. This work used both experimental and mathematical modeling approaches.

The results of this work are: (1) investigative results concerning sorption of typical, organic contaminants to a coastal North Carolina subsurface material; (2) the derivation and development of numerical models suitable for simulating contaminant migration in the subsurface; and (3) a dimensionless analysis that shows criteria under which sorption rate and equilibrium considerations yield prolonged cleanup times.

PREVIOUS RESEARCH

The sorption-desorption process is one of the most important processes influencing contaminant movement in subsurface systems. Sorption is the inter-phase mass transfer of a solute from the groundwater phase to the solid phase; desorption is the inter-phase mass transfer of a solute from the solid phase to the groundwater phase. Like all inter-phase, mass-transfer processes, the sorption-desorption process can be defined by the final phase equilibrium of the solute between the two respective phases and the time required to approach that final equilibrium.

A large body of literature exists describing experimental observations of sorption equilibria between soils and sediments for a wide variety of organic and inorganic compounds (Bailey and White, 1970; Pierce et al., 1971; Hamaker and Thompson, 1972; Browman and Chesters, 1975; Karickhoff et al., 1979; Kenaga and Goring, 1980; Morrill et al., 1982; Murali and Aylmore, 1983; Voice and Weber, 1983; Karickhoff, 1984; Chiou, 1986). This work has led to a maturing of the current level of understanding of the sorption-desorption process, from both a predictive and a mechanistic perspective. It is well understood that sorption to soils (or sediments) is a function of several variables: ionic nature of the solute; polarity of the solute; solvency of the solute with respect to the solvent; presence of competing solutes; organic carbon content of the solid; mineral content of the solid; system pH; temperature; and ionic strength of the solvent.

Much of the recent research has dealt with the sorption and desorption of neutral, hydrophobic organic compounds to soils and sediments (Karickhoff et al., 1979; Chiou et al., 1983; Karickhoff, 1984; Gschwend and Wu, 1985; Miller and Weber, 1986; Woodburn et al., 1986). It is currently understood that the fraction of organic matter of a soil or sediment is the dominant characteristic that influences the sorption of a given neutral, low polarity, hydrophobic, organic compound from an aqueous solution. Further, there is significant evidence to suggest that sorption for such systems is a partitioning like phenomenon—or

an absorption of the organic solute into the organic matter of the soil or sediment.

Unfortunately, little work has been done on typical aquifer solids that have very low (less than 0.1 percent) total organic carbon content. The work that has been done with low organic carbon materials suggests that mineral surface sorption may be important for typical aquifer solids systems (Banerjee et al., 1980; Means et al., 1980, and 1982; Mingelgrin and Gerstl, 1983; Goltz and Roberts, 1986; Mackay et al., 1986; Stauffer and MacIntyre, 1986).

Definition of the sorption-desorption, mass-transfer process also requires a determination of the rate at which equilibrium is approached. Many investigations have assumed that the sorption-desorption process may be approximated as an instantaneous, local equilibrium between the solid and the aqueous phase (Back and Cherry, 1976; Anderson, 1979; Freeze and Cherry, 1979; Faust and Mercer, 1980; Prickett et al., 1981; Roberts et al., 1982). However, the literature substantiates that rates of sorption-desorption are important for many organic solute/solid systems (Kay and Elrick, 1967; Leenheer and Ahlrichs, 1971; Boucher and Lee, 1972; Karickhoff, 1980; Hutzler et al., 1984, and 1986; Karickhoff, 1984; Miller, 1984; Miller and Weber, 1984a, 1984b, 1986, and 1988; Coates and Elzerman, 1986; Crittenden et al., 1986; Weber and Miller, 1988; Wu and Gschwend, 1986). Recent work has described the relationship among sorption-desorption rates, solute source function, and system hydrodynamics (Valocchi, 1985, and 1986; Parker and Valocchi, 1986). It is now understood that the sorption-desorption process may require months to years to achieve "true equilibrium" in some hydrophobic solute-soil systems (Coates and Elzerman, 1986; Miller and Weber, 1986, and 1988; Weber and Miller, 1988).

Of additional concern, for the description of the sorption-desorption process, is the influence that multiple solute component (multi-component) systems have on both system equilibrium and the rate of sorption-desorption. The behavior of multi-component systems is important to understand because most cases of subsurface contamination include more than one solute constituent. However, relatively few studies have investigated

multi-component sorption-desorption (Boyd, 1982; Chiou et al., 1983; Coates and Elzerman, 1986; Weber et al., 1986). The small amount of work that has been done suggests that competition exists between solutes at equilibrium with the solid phase, especially for high solute concentrations—typical of regions of many subsurface contamination sites (Boyd, 1982; Coates and Elzerman, 1986; Weber et al., 1986). Of additional interest is the recent finding that multi-component systems of PCB's and river sediments desorbed at a rate which was 60 percent slower than a similar single component system (Coates and Elzerman, 1986).

MATERIALS AND METHODS

MATERIALS

The subsurface material used in this investigation was collected from a research site located at Tarawa Terrace on Marine Corps Base Camp Lejeune. The hydrogeology and details of this site have been discussed in a previous publication (DiGiano et al., 1988) and will not be repeated here. Solid materials used in this investigation were collected from an uncontaminated portion of the aquifer in a relatively uniform horizon, between 25 to 35 feet below ground surface. The material collected was air dried and well-mixed to form a single composite sample. The composite material was analyzed using standard methods for the physical characteristics of grain size by sieving, and density by a mass per volume displacement method. Standard methods were used to measure the chemical characteristics of pH (Mitchell, 1976), organic carbon fraction (American Public Health Association, 1986), and cation exchange capacity (Black, 1965). The physical and chemical characteristics determined for the Camp Lejeune sample are summarized in Table 1, while a grain-size distribution diagram is shown by Figure 1.

The Camp Lejeune subsurface sample investigated was a highly-uniform, medium-fine sand, which has a typical particle density. Further, the Camp Lejeune sample is acidic in nature, has a low cation exchange capacity, and an extremely low total organic carbon content. It is expected, based upon the above referenced analysis, that the Camp Lejeune sample investigated is not atypical of near-surface, coastal North Carolina subsurface materials.

The solutes investigated in this study were p-dichlorobenzene, toluene, and o-xylene. The physical and chemical characteristics of these solutes are summarized in Table 2. Toluene and o-xylene were chosen because they are common aromatic constituents in gasoline, therefore common groundwater contaminants at many locations in North Carolina

Table 1. Solid Material Characteristics

Parameter	Value
Median Grain Size	0.251 mm
Uniformity Coefficient (d_{60}/d_{10})	1.57
Particle Density (ρ)	2.64 g/cc
pH	5.3
Organic Carbon Fraction (f_{oc})	0.024 %
Standard Deviation (σ_x)	0.0024%
Cation Exchange Capacity	5.52 meq/100 g
Standard Deviation (σ_x)	0.98 meq/100 g

and across the United States. These solutes are only moderately hydrophobic and are considered volatile. For this reason, p-dichlorobenzene was also used in this investigation because it is similar to the other compounds in structure and properties, yet is somewhat more hydrophobic and less volatile. These features were expected to make experimental determination of sorption properties somewhat easier, while maintaining relevance to the most common problem of groundwater contamination in the State.

Experimental solutions were comprised of distilled-deionized water that included a 0.005 M borate buffer to regulate pH, and 0.01 N calcium chloride to aid in phase separation, by destabilizing colloidal particles. Potential biodegradation was avoided by including 0.015 M sodium azide in all experimental solutions—a proven method (Fletcher and Kaufman, 1980; Kale and Raghu, 1982).

SOLUTE EXTRACTION AND MEASUREMENT METHODS

Two types of solute measurements were made during this project: inorganic chloride concentrations; and organic solute concentrations of p-dichlorobenzene, toluene, and

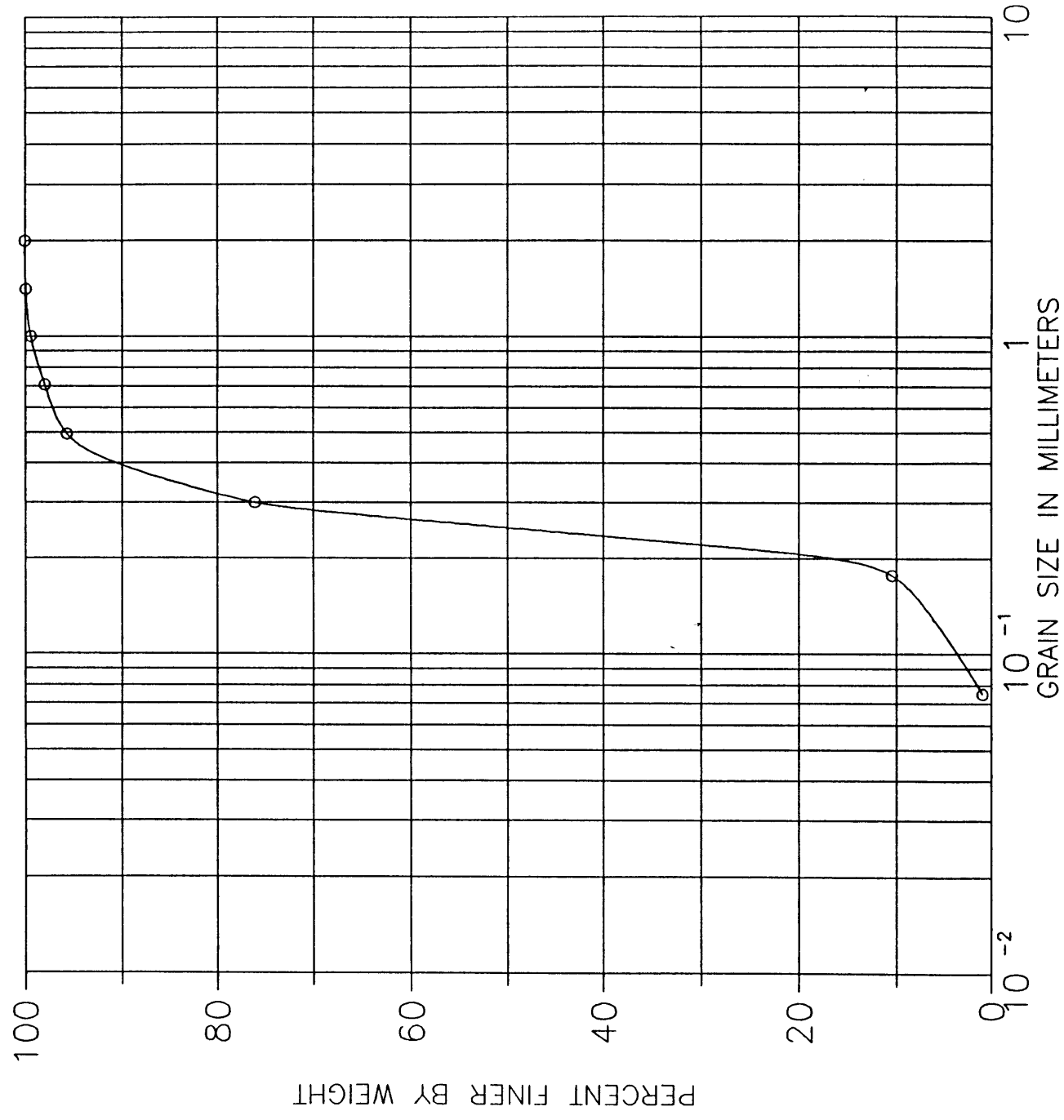


Figure 1. Grain-size distribution for Camp Lejeune subsurface material.

Table 2. Solute Properties

Parameter	p-Dichlorobenzene	Toluene	o-Xylene
Molecular Weight (g/mole)	147.01	92.10	106.17
Melting Point (°C)	53.0	-95.1	-25.0
Boiling Point (°C)	173.4	110.8	144.4
Specific Gravity (at 20°C)	1.458	0.867	0.880
Aqueous Solubility (mg/l)	4.9 x 10 ¹ at 22. °C 7.9 x 10 ¹ at 25. °C	4.70 x 10 ² at 16. °C 5.15 x 10 ² at 20. °C	1.75 x 10 ² at 25. °C
Log <i>K_{ow}</i> (median) ^a	3.38	2.71	2.93
Vapor Pressure (mm Hg)	6.0 x 10 ⁻¹ at 20. °C 1.8 x 10 ⁰ at 30. °C	1.0 x 10 ¹ at 6.4°C 2.2 x 10 ¹ at 20. °C 4.0 x 10 ¹ at 31.8°C	5.0 x 10 ⁰ at 20. °C 6.6 x 10 ⁰ at 25. °C 9.0 x 10 ¹ at 30. °C ^c
Henry's Constant (<i>H_c</i>)	1.4 x 10 ⁻¹ at 20. °C ^b	2.81 x 10 ⁻¹ at 20. °C	2.2 x 10 ⁻¹ at 25. °C

General Reference: Verschueren (1983)

^a Hansch and Leo (1979)

^b Lyman et al. (1982)

^c Boublik et al. (1975)

o-xylene. Chlorides were measured using a standard silver nitrate titration method (American Public Health Association, 1986).

Organic solute analysis was performed using liquid-liquid extraction, followed by capillary gas chromatography. Samples were extracted by combining an aqueous sample with the organic solvent hexane in 25-ml Pierce vials with minimal headspace. The vial and its contents were thoroughly mixed and allowed a minimum of several hours to equilibrate. The solute 1,2,4- trichlorobenzene was included in the hexane and carried along as an internal standard for analysis of p-dichlorobenzene, while octane was used as an internal standard for analysis with toluene and o-xylene.

Solute mass was analyzed using a Varian 3700 high-resolution GC with a flame ionization detector (FID). Chromatographic separation was achieved on a 30-m, Supelco SPB-1 fused-silica capillary column with splitless injection and temperature programming: the initial temperature was held at 35°C for 8 minutes, and then programmed to 175°C at a rate of 6°C per minute. The injector temperature was set at 285°C and the FID was set at 300°C; and the helium carrier gas flow rate was 1.7 ml per min.

A standard curve of the target compounds was determined to relate integrated peak area to mass of solute for each set of aqueous samples. This was accomplished by regressing analyte area normalized by the internal standard area (analyte response factor) as a function of analyte concentration. This analysis method yielded a linear relationship with high correlation coefficients (usually exceeding 0.99).

BOTTLE-POINT EXPERIMENTAL METHODS

Bottle-point reactors (BPR's) were used to measure the rate of sorption-desorption by placing a known and equal amount of solid in borosilicate centrifuge bottles, adding a constant volume of solution of a known solute concentration to each bottle—yielding nearly headspace-free conditions, and tumbling all bottles to maintain well-mixed conditions. The BPR's were removed from the tumbler and centrifuged for separation of the

solid and aqueous phases at different times during the course of the study. At each of these times, the solution-phase solute concentration was measured and the solid-phase solute concentration was calculated by difference from the initial mass of solute present. Blanks—BPR's with no solid phase—were carried along to determine sample-handling, volatilization, and extraction errors associated with the procedure.

Sorption equilibrium experiments were performed using a bottle-point-reactor method similar to the rate-study method. The chief differences were dictated by the objective: to determine the equilibrium solid-phase concentration as a function of the fluid-phase concentration—for a wide-range of fluid-phase concentrations. To meet this objective, the initial fluid-phase concentration was varied over a wide range, and three weeks were allowed for equilibration between the phases. After tumbling the bottle to maintain well-mixed conditions for the equilibration period: phase separation was accomplished by centrifugation; the fluid-phase concentration was measured; and the solid-phase concentration was calculated by attributing the reduction in solute mass in the solution phase to sorption. Blanks were carried along to determine sample handling, volatilization, and extraction errors associated with the procedure.

COLUMN-REACTOR EXPERIMENTAL METHODS

Figure 2 shows a schematic illustration of the column-reactor system used to investigate sorption characteristics in the presence of the hydrodynamic transport processes of advection and dispersion. Borosilicate glass and stainless steel were used for all parts that were in contact with the solute-carrying solution to minimize extraneous sorption. The column-reactor experimental apparatus used was a 2.4-cm diameter glass column. A stainless-steel piston pump provided a constant flow to the column, with adjustments in flow rate accomplished by varying the length of the piston stroke.

The column was packed by enclosing subsurface material between 1.5-cm end layers of glass beads to prevent particle migration from the column. Concentrations were monitored

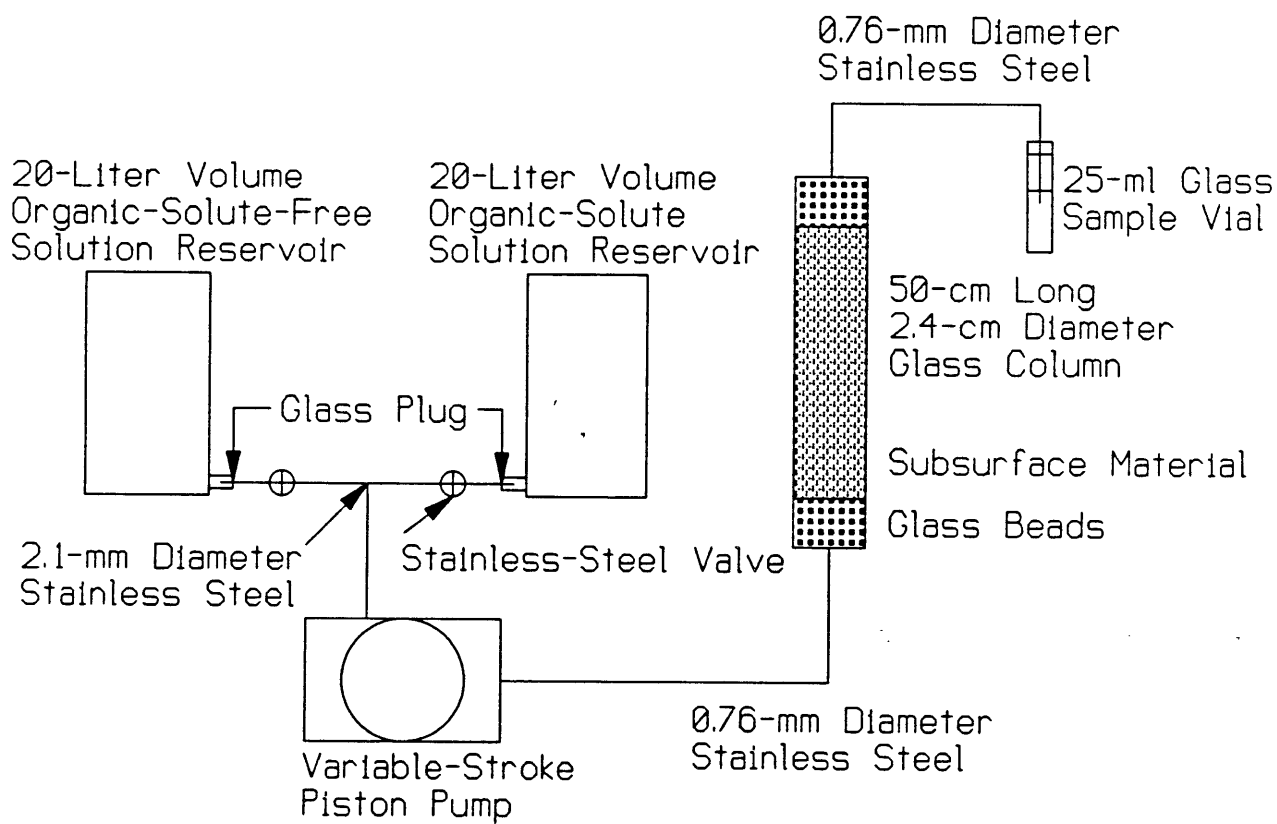


Figure 2. Column-reactor system.

by discrete sampling of the column influent and effluent streams. Chloride was used as a nonreactive tracer to determine the hydrodynamic characteristics of the packed column. This was accomplished by first equilibrating a column with a flow of an organic-free feed solution and then introducing a solution that contained about 3.2 mg/l of toluene, 3.4 mg/l of o-xylene, and 0.01 N calcium chloride. Differences between the movement of the chloride solute and the organic solutes were attributed to organic solute sorption to the subsurface material in the column.

MATHEMATICAL MODELING

GENERAL

The purpose of this research was to investigate the effect of organic solute sorption and desorption on aquifer restoration using mathematical modeling. While the results of the modeling analysis are the chief practical benefit of this work, it is necessary for completeness to describe the modeling approaches considered, and the solution procedures used. This section presents a narrative explanation of the modeling approaches considered, and a brief development of the mathematical equations used. The details of the numerical approximation methods used are included as appendix sections to this report, because they were considered of less general interest than the conceptual basis and governing equation framework presented in this section. Rigorous validations of all mathematical models using both analytical solutions and mass-balance approaches have been completed. These results are not presented in this document, but citations to the refereed literature, at appropriate locations in the model derivations, are offered as evidence of model validity .

This section briefly outlines three classes of models considered: equilibrium sorption models, sorption-rate models, and advective-dispersive-reactive (ADR) models. These models are listed in order of increasing complexity, with each model class including a member of the previous model class or classes. For example, complete specification of a sorption-rate model requires a specification of an equilibrium sorption model. Similarly, a complete specification of an ADR model requires specification of an equilibrium sorption model and a sorption-rate model.

SORPTION EQUILIBRIUM MODELS

When an organic solute exists in a natural system comprised of multiple phases, the organic solute is distributed among the phases present. Given sufficient time, the solute distribution among the phases present will approach an equilibrium condition—if no solute

is added to or removed from the system, and if solute reactions do not occur.

The system under consideration in this report consists of two phases: an aqueous phase, and a subsurface solid phase. The introduction of an organic solute in the aqueous phase of the subsurface environment leads to mass transfer of solute from the fluid phase to the solid phase. The equilibrium distribution of solute between the solid phase and the aqueous phase may be studied using laboratory methods, like the bottle-point reactor methods described previously. Several models exist that describe the solid-phase solute concentration as a function of the aqueous-phase solute concentration at equilibrium. These models are often called sorption equilibrium isotherm models or sorption equilibrium models for short. Three common sorption equilibrium models are considered here: the linear model, the Freundlich model, and the Langmuir model.

The most common sorption equilibrium model is the linear model

$$q_e = K_p C_e \quad (1)$$

where: q_e is the equilibrium, mass-average solid-phase concentration—defined as the mass of solute per mass of solid phase; K_p is a linear sorption equilibrium coefficient; and C_e is the volume-average, fluid-phase solute concentration at equilibrium.

The linear equilibrium model is appealing because of the simplicity of sorption modeling based upon it. This will be shown in later subsections of this report. A further appeal of the linear equilibrium model is the considerable body of literature reporting linear sorption equilibrium coefficients, and the existence of several constitutive methods (or correlation methods) for predicting linear sorption equilibrium coefficients based upon solute and solid properties (Sabljčić, 1987). Frequent solute properties correlated to equilibrium sorption are the octanol:water partition coefficient (K_{ow}), the aqueous solubility (S), and the molecular connectivity index (χ). The most frequently correlated solid material properties relating to organic solute sorption are the fraction of organic carbon (f_{oc}), or

the fraction of organic matter content (f_{om}) of the natural solid material. The actual form of these constitutive expressions is not central to the discussion of this section—noting the existence of such expressions is important. Constitutive methods for predicting linear sorption equilibrium coefficients are discussed in greater detail in the Discussion section of this report.

The equilibrium sorption relationship between an organic solute in the fluid phase and a natural solid phase has often been reported as being nonlinear (Hamaker and Thompson, 1972; Weber and Miller, 1989). For such instances, alternate equilibrium models have been used. The Freundlich sorption equilibrium model is one of the most frequently used of these models

$$q_e = K_F C_e^{n_F} \quad (2)$$

where K_F is the sorption capacity constant and n_F is the sorption intensity constant. Typical values of n_F for subsurface solid materials and organic solutes range from 0.7 to 1.0—a slightly concave relationship. The Freundlich model is empirically founded, but it is widely used in practice.

Another common nonlinear sorption equilibrium model is the Langmuir sorption equilibrium model. The Langmuir model can be derived from thermodynamic or chemical kinetic principles and is of the form

$$q_e = \frac{Q^\circ b C_e}{1 + b C_e} \quad (3)$$

where Q° is a constant representing the maximum solid-phase solute concentration approached while b is a sorption energy-related constant.

SORPTION RATE SUB-MODELS

Batch-Reactor Model

In addition to equilibrium considerations, the distribution of an organic solute between the aqueous phase and the solid phase depends upon the rate at which mass transfer occurs between the phases (i.e. the nature of the rate of approach to equilibrium). Differences in the rate of sorption or desorption can lead to profound differences in the spatial distribution of a contaminant in the subsurface at a given time, and correspondingly to a system's response to clean-up efforts.

Sorption rate sub-models can be presented in a batch-reactor (or closed-system) framework with the mass-balance expression

$$\frac{dC}{dt} = -\frac{M}{V} \frac{dq}{dt} + \left(\frac{dC}{dt} \right)_{rxn} + \Gamma(C) \quad (4)$$

where: t is time; M is the mass of the solid phase; V is the volume of the solution; the subscript rxn denotes chemical or biological reactions; and $\Gamma(C)$ is a solute source function—an addition of a mass of solute per unit volume of solution in the closed system per unit time. It should be noted that the sign convention used in Equation 4 for reactions assumes a reaction that increases the mass of solute in the system.

For a closed system, sorption rate sub-models enter equation 4 by specifying a rate of change of the solid-phase solute concentration as a function of time, or dq/dt .

Two-Site Model

The two-site model is based upon the concept that the solid surface contains two types of sorption sites, fast sites and slow sites. Sorption occurs quickly on the fast sites, and the solute concentration in the fluid-phase and on the fast sites is assumed to be in equilibrium. For the slow sites, sorption occurs at a first-order rate, or as a function of the difference between the solid-phase solute concentration at equilibrium and the solid-phase

solute concentration at a given time on the slow sites. After a sufficiently long period of time (the actual time is system dependent), the fluid-phase solute concentration and the overall solid-phase solute concentration approach an equilibrium.

The first step in specifying a complete two-site model is the selection of an equilibrium expression for the fast and slow sites. For the case where both fast- and slow-site sorption equilibrium may be described using a Freundlich sorption-equilibrium model, the following expressions describe the overall equilibrium between the fluid and solid phases

$$\begin{aligned} q_e &= q_{fe} + q_{se} \\ &= K_f C_e^{n_f} + K_s C_e^{n_s} \end{aligned} \quad (5)$$

where: q_{fe} is the mass-average solid-phase solute concentration of the fast sites at equilibrium; q_{se} is the mass-average solid-phase solute concentration of the slow sites at equilibrium; K_f is the Freundlich sorption-equilibrium model coefficient for the fast sites; n_f is the Freundlich sorption-equilibrium model exponent for the fast sites; K_s is the Freundlich sorption-equilibrium model coefficient for the slow sites; and n_s is the Freundlich sorption-equilibrium model exponent for the slow sites.

The two-site rate model may be expressed as

$$\frac{dq}{dt} = \frac{dq_f}{dt} + \frac{dq_s}{dt} \quad (6)$$

where q_f is the solid-phase solute concentration of the fast sites, and q_s is the solid-phase solute concentration of the slow sites. Since the fast sites are assumed to be in equilibrium with the fluid-phase solute concentration, the dependent variable q_f may be eliminated by using the chain rule

$$\frac{dq_f}{dt} = \frac{dq_f}{dC} \frac{dC}{dt} \quad (7)$$

where

$$\frac{dq_f}{dC} = n_f K_f C^{n_f-1} \quad (8)$$

follows from the equilibrium description of the fast sites. Including the first-order model to describe sorption to the slow sites gives

$$\frac{dq}{dt} = n_f K_f C^{n_f-1} \frac{dC}{dt} + \alpha (K_s C^{n_s} - q_s) \quad (9)$$

Substituting Equation 9 into 4 gives the fluid-phase equation for the two-site model

$$R_{bf} \frac{dC}{dt} = -\frac{M}{V} \alpha (K_s C^{n_s} - q_s) + \left(\frac{dC}{dt} \right)_{rxn} + \Gamma(C) \quad (10)$$

where the retardation factor for the fast sites in a batch reactor is given by

$$R_{bf} = 1 + \frac{M n_f K_f}{V} C^{n_f-1} \quad (11)$$

Equation 10 has two dependent variables, since the solute concentration on the slow sites changes as a function of time. Therefore, an equation for the solute concentration on the slow sites is needed and is of the form

$$\frac{dq_s}{dt} = \alpha (K_s C^{n_s} - q_s) + \left(\frac{dq_s}{dt} \right)_{rxn} + \Gamma(q_s) \quad (12)$$

where $\Gamma(q_s)$ is a solute source function for the slow solid-phase sites.

Solution of the batch reactor sorption problem requires simultaneous solution of equations 10 and 12. These equations are still in a general form because the reaction terms and source functions have not been specified. For the special case where solute degradation occurs by a first-order mechanism from both the fluid and solid phase and the only source

of solute is through an initial addition (or in mathematical vernacular an initial condition), the two-site model for a batch reactor may be written as

$$R_{bf} \frac{dC}{dt} = -\frac{M}{V} [k_{sd}K_f C^{n_f} + \alpha (K_s C^{n_s} - q_s)] - k_{fd}C \quad (13)$$

and

$$\frac{dq_s}{dt} = \alpha (K_s C^{n_s} - q_s) - k_{sd}q_s \quad (14)$$

for the initial conditions

$$\begin{aligned} M_s &= VC_0 + MK_f C_0^{n_f} \\ q_s(t=0) &= 0 \end{aligned} \quad (15)$$

where: k_{sd} is a first-order decay rate for solute on the solid phase; k_{fd} is a first-order decay rate for solute in the fluid phase; M_s is the mass of the solute initially added to the system; and C_0 is the fluid-phase concentration at $t = 0$.

A FORTRAN computer code was written to solve the two-site sorption model in a closed system, which is described by equations 13 to 15. The two-site model was solved by using the Newton-Raphson method to solve for the initial condition, while the coupled ordinary differential equations were solved using Gear's method (1971). The derived model was validated by comparison to published results of a less general two-site model (Weber and Miller, 1988).

Dual-Resistance Model

Diffusion models have been applied to describe transport phenomena for a variety of boundary conditions and conceptual process variations in rock systems (Neretnieks, 1980; Rasmuson and Neretnieks, 1980; Rasmuson, 1981; Rasmuson et al., 1982) and in porous media systems (Van Genuchten and Wierenga, 1976, 1977; Van Genuchten et al., 1977;

Valocchi, 1985; Crittenden et al., 1986; Goltz and Roberts, 1986; Hutzler et al., 1986). These diffusion modeling approaches have relied upon physical interpretations of the process; chiefly the concept that one portion of media void space fluid is mobile, and another portion is immobile. This approach, while able to describe the tailing frequently observed in solute concentration breakthrough curves (BTCs), still relies upon the assumption that the solid phase and the solution phase are always in solute sorption equilibrium. Data collected in batch reactors have shown that sorption can occur slowly, frequently extending over periods of several days (Miller and Weber, 1986) or even much longer (Karickhoff, 1980). The slow rate of the sorption process has been attributed to either an intraparticle diffusion process (Karickhoff, 1980) or a dual-resistance process involving boundary layer and intraparticle diffusion (Miller, 1984; Miller and Weber, 1984b, 1986, 1988; Weber and Miller, 1988).

The dual-resistance model describes sorption as a series of mass-transfer steps that are illustrated by Figure 3: molecular diffusion through a hydrodynamic boundary layer surrounding a solid particle; and diffusion within the particle itself. It is unlikely that the diffusion process occurs uniformly through an entire subsurface solid particle. Instead it probably occurs through agglomerations of organic material associated with the particle. The difference between the mechanistic concept and physical reality does not limit the practical application of the dual-resistance model because the mass average of the solid-phase solute concentration is the macroscopic property that affects the observed fluid-phase concentration.

For spherical solid particles, the dual-resistance model can be expressed as a generalized form of Fick's second law of diffusion in spherical coordinates

$$\frac{\partial q_r}{\partial t} = \frac{D_s}{r^2} \frac{\partial}{\partial r} \left(r^2 \frac{\partial q_r}{\partial r} \right) + \left(\frac{\partial q_r}{\partial t} \right)_{rzn} + \Gamma(q_r) \quad (16)$$

with the boundary and initial conditions

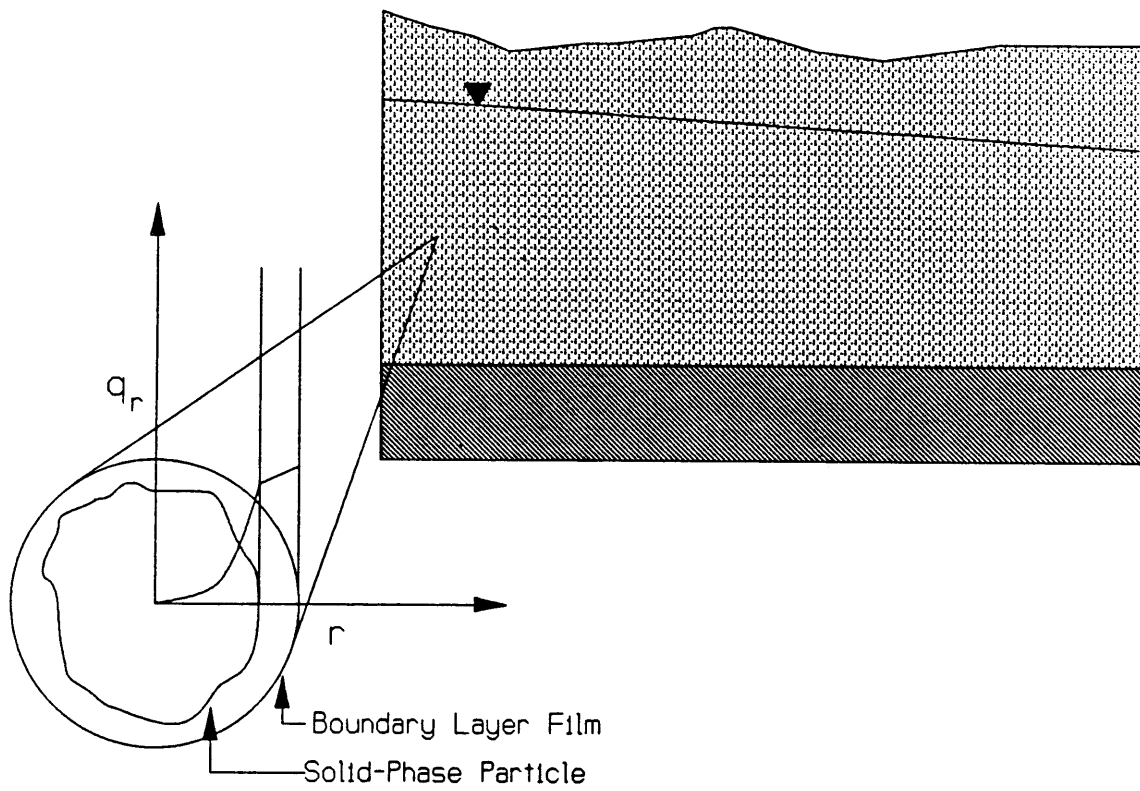


Figure 3. Dual-resistance model.

$$\left. \frac{\partial q_r}{\partial r} \right|_{r=R} = \frac{k_f}{D_s \rho} (C - C_s) \quad (17)$$

$$\left. \frac{\partial q_r}{\partial r} \right|_{r=0} = 0 \quad (18)$$

$$q_r(0 \leq r \leq R, t = 0) = 0 \quad (19)$$

where q_r is the solid-phase solute concentration as a function of radial position r ; D_s is an intraparticle diffusion coefficient; k_f is a film mass-transfer coefficient; C_s is the fluid-phase solute concentration at equilibrium with the solid-phase solute concentrations at the exterior of the particle; ρ is the density of the solid; and R is the solid particle radius. The Freundlich model is used to specify the assumed equilibrium that relates $q_r(r = R)$ to C_s at the exterior of the solid particle.

Equation 17 is a boundary condition that requires the mass of solute that moves across the film for a given time be equivalent to the mass of solute that enters the exterior of the solid particle. This is equivalent to saying that no accumulation of mass occurs within the fluid film. Equation 18 is the boundary condition for the interior of solid particle, which follows directly from the assumption of spherical symmetry. Equation 19 is simply the initial condition, which states that the solid-phase solute concentration is 0 initially for all locations in the solid phase.

The instantaneous rate of sorption at any time may be derived from mass-balance considerations of flux through the fluid film, giving

$$\left(\frac{dq}{dt} \right)_{srp} = \frac{3k_f}{R\rho} (C - C_s) \quad (20)$$

Substituting Equation 20 into Equation 4 gives

$$\frac{dC}{dt} = -\frac{3k_f M}{RV\rho} (C - C_s) + \left(\frac{\partial C}{\partial t} \right)_{rxn} + \Gamma(C) \quad (21)$$

For the case of a solute that enters the system as an initial condition only and degrades according to a first-order process from both the fluid and solid phases, the fluid-phase equation becomes

$$\frac{dC}{dt} = -\frac{3k_f M}{RV\rho}(C - C_s) - k_{fd}C \quad (22)$$

and the solid-phase equation is

$$\frac{\partial q_r}{\partial t} = \frac{D_s}{r^2} \frac{\partial}{\partial r} \left(r^2 \frac{\partial q_r}{\partial r} \right) - k_{sd}q_r \quad (23)$$

while the boundary and initial condition expressed by Equations 17 to 19 remain the same.

The solution of the dual-resistance model is somewhat more difficult than the two-site model, yet straightforward. The solution is nonlinear, because the Freundlich sorption-equilibrium model is used to couple the ordinary differential equation for the fluid-phase solute concentration (Equation 22) to the partial differential equation for solid-phase solute concentration (Equation 23). A sixth-order Galerkin finite element method was used to reduce the spatial derivatives of the solid-phase equation to a set of algebraic equations, while the system of ordinary differential equations was then solved using Gear's algorithm (1971). The details of this method are summarized in Appendix I. Validation of the solution accuracy has been accomplished by comparison to an available analytical solution (Pedit and Miller, 1988).

ADVECTIVE-DISPERSIVE-REACTIVE EQUATION MODELING

General Advective-Dispersive-Reactive Equation

The physics that govern the movement of contaminants in the subsurface are well-known (e.g. Bear, 1979; de Marsily, 1986) and will not be derived in detail in this report. In general, solute transport occurs: with the bulk movement of groundwater, or by advection;

and by deviations from the bulk movement, or by mechanical dispersion. Chemical and biological processes also occur in the subsurface and need to be considered in any general statement of reactive transport in the subsurface. A general form of the ADR equation is given as

$$\frac{\partial C}{\partial t} = \text{div} (\mathbf{D}_h \text{grad } C) - \vec{v} \cdot \text{grad } C + \left(\frac{\partial C}{\partial t} \right)_{rxn} + \Gamma(C) \quad (24)$$

where: D_h is a second-rank, symmetrical hydrodynamic dispersion tensor; and \vec{v} is the mean macroscopic pore velocity vector of the aqueous phase.

For flow in a one-dimensional system with a constant velocity and dispersion, Equation 24 may be simplified to

$$\frac{\partial C}{\partial t} = D_x \frac{\partial^2 C}{\partial x^2} - v_x \frac{\partial C}{\partial x} + \left(\frac{\partial C}{\partial t} \right)_{rxn} + \Gamma(C) \quad (25)$$

where: D_x is the hydrodynamic dispersion coefficient in the x direction; and v_x is the average macroscopic fluid-phase velocity in the x direction.

The one-dimensional cartesian-coordinate form of the ADR equation is appropriate when the flow of groundwater is linear in the x direction, and when a concentration gradient exists in only the x direction. Such conditions prevail under controlled laboratory conditions, like flow through a column reactor. Such conditions may also be approximated under field conditions where the source of the contaminant is spatially extensive, which ideally means a plane source of contaminant that fully penetrates an aquifer and is infinitely long in the horizontal direction transverse to the direction of mean flow, y .

One-Dimensional Local-Equilibrium Model

A common method of including sorption in the advection-dispersion-reaction (ADR) equation is the local-equilibrium model. This approach can be developed by first considering the one-dimensional form of the ADR equation for a sorbing solute, which undergoes

first-order degradation from the fluid and solid phases and has no internal source of solute within the domain

$$\frac{\partial C}{\partial t} = D_x \frac{\partial^2 C}{\partial x^2} - v_x \frac{\partial C}{\partial x} + \left(\frac{\partial C}{\partial t} \right)_{srp} - k_{fd} C \quad (26)$$

where the subscript *srp* indicates solute lost from the fluid phase as a result of sorption to the solid phase.

If the fluid and solid phases are assumed to always be in equilibrium then the chain rule can be used to relate the fluid- and solid-phase solute concentrations by

$$\frac{\partial q}{\partial t} = \frac{\partial q}{\partial C} \frac{\partial C}{\partial t} \quad (27)$$

Combining equations 26 and 27, and including a solid-phase decay term gives

$$R_f \frac{\partial C}{\partial t} = D_x \frac{\partial^2 C}{\partial x^2} - v_x \frac{\partial C}{\partial x} - k_{fd} C - \frac{\rho_b k_{sd}}{n} q \quad (28)$$

where the retardation factor is defined as

$$R_f = 1 + \frac{\rho_b}{n} \frac{\partial q}{\partial C} \quad (29)$$

For the case where the sorption equilibrium between the fluid and solid phases is described by the Freundlich model, Equations 28 and 29 may be written as

$$R_f \frac{\partial C}{\partial t} = D_x \frac{\partial^2 C}{\partial x^2} - v_x \frac{\partial C}{\partial x} - k_{fd} C - \frac{\rho_b k_{sd}}{n} K_F C^{n_F} \quad (30)$$

$$R_f = 1 + \frac{\rho_b}{n} n_F K_F C^{n_F-1} \quad (31)$$

For the case where the sorption equilibrium between the fluid and solid phases is described by the linear isotherm, Equations 28 and 29 may be written as

$$R_f \frac{\partial C}{\partial t} = D_x \frac{\partial^2 C}{\partial x^2} - v_x \frac{\partial C}{\partial x} - k_{fd} C - \frac{\rho_b k_{ad}}{n} K_p C \quad (32)$$

$$R_f = 1 + \frac{\rho_b}{n} K_p C \quad (33)$$

For the linear, local-equilibrium assumptions R_f is a constant if spatial variability is not considered. This means that any solution of the ADR equation can be extended to account for linear, local-equilibrium sorption with appropriate adjustment by the constant R_f . For the case where the isotherm model is nonlinear, R_f becomes a function of C and the ADR equation is nonlinear. The numerical solution method used to solve the local-equilibrium model will be discussed in the following sub-section and in Appendix II. It will be shown that the local-equilibrium model is a subset of the two-site model.

One-Dimensional, Two-Site Model

Descriptions of two-site ADR models in the literature differ in conceptualization of associated reactions and their reduction to equation form; both classical pseudo-homogeneous-phase chemical kinetic and heterogeneous mass-transfer derivations are possible (Selim et al., 1976; Cameron and Klute, 1977; Karickhoff, 1980; Miller, 1984; Miller and Weber, 1986). The two-site ADR model may be derived by simply substituting the two-site sorption-rate sub-model previously derived into the general one-dimensional form of the ADR equation. This process extends the local-equilibrium model by adding a second sorption component, which occurs at a first-order rate.

Consider the one-dimensional ADR equation for a sorbing solute, which undergoes first-order degradation from the fluid and solid phase and has no internal source of solute within the domain

$$\frac{\partial C}{\partial t} = D_x \frac{\partial^2 C}{\partial x^2} - v_x \frac{\partial C}{\partial x} + \left(\frac{\partial C}{\partial t} \right)_{srp} - k_{fd} C \quad (34)$$

For the two-site model the sorption term may be expanded into fast and slow components giving

$$\left(\frac{\partial C}{\partial t} \right)_{srp} = -\frac{\rho_b}{n} \left[\frac{\partial q_f}{\partial t} + k_{sd} q_f + \left(\frac{\partial q_s}{\partial t} \right)_{srp} \right] \quad (35)$$

Using the Freundlich model for fast-sites gives

$$R_f \frac{\partial C}{\partial t} = D_x \frac{\partial^2 C}{\partial x^2} - v_x \frac{\partial C}{\partial x} - \frac{\rho_b}{n} \left[k_{sd} K_f C^{n_f} + \left(\frac{\partial q_s}{\partial t} \right)_{srp} \right] - k_{fd} C \quad (36)$$

$$R_f = 1 + \frac{\rho_b}{n} n_f K_f C^{n_f - 1} \quad (37)$$

Substituting the first-order rate portion of the two-site model into Equation 36 for $(\partial q_s / \partial t)_{srp}$ gives

$$R_f \frac{\partial C}{\partial t} = D_x \frac{\partial^2 C}{\partial x^2} - v_x \frac{\partial C}{\partial x} - \frac{\rho_b}{n} [k_{sd} K_f C^{n_f} + \alpha (K_s C^{n_s} - q_s)] - k_{fd} C \quad (38)$$

Equation 38 has two dependent variables C and q_s . Therefore, it is necessary to form a second equation, which describes the solute concentration on the slow sites of the solid phase. This requirement is met by specifying an ordinary differential equation for each spatial location in the domain of the form

$$\frac{dq_s}{dt} = \alpha (K_s C^{n_s} - q_s) - k_{sd} q_s \quad (39)$$

It is worth noting that Equation 39 is identical to the batch-reactor form of the slow-site solid-phase equation.

A FORTRAN program was derived to solve Equations 38 and 39 subject to the boundary conditions

$$C(t > 0, x = 0) = C_0 \quad (40)$$

$$\left. \frac{\partial C}{\partial x} \right|_X = 0 \quad (41)$$

and the initial conditions

$$C(t = 0, x) = 0 \quad (42)$$

$$q_s(t = 0, x) = 0 \quad (43)$$

where X is the length of the domain.

The finite difference method was used to reduce the fluid-phase ADR equation to a system of ordinary differential equations in time. This system of equations was solved simultaneously along with the system of ordinary differential equations describing the solute concentration on the slow-site portion of the solid phase using Gear's algorithm (1971). Additional details of this numerical approximation procedure are presented in Appendix II. The FORTRAN code constructed to solve this problem was validated by comparison to an available analytical solution (Cameron and Klute, 1977; Miller and Weber, 1988), which is valid for the case of a linear sorption-equilibrium model.

One-Dimensional, Dual-Resistance Model

The dual-resistance sorption-rate sub-model may be included in the ADR equation along with a Freundlich sorption-equilibrium model. For a solute that enters the domain only at the inlet boundary of the domain and undergoes first-order degradation from the fluid and solid phase, the fluid-phase ADR equation is

$$\frac{\partial C}{\partial t} = D_x \frac{\partial^2 C}{\partial x^2} - v_x \frac{\partial C}{\partial x} - \frac{3(1-n)k_f}{nR} (C - C_s) - k_{fd}C \quad (44)$$

the solid-phase equation is

$$\frac{\partial q_r}{\partial t} = \frac{D_s}{r^2} \frac{\partial}{\partial r} \left(r^2 \frac{\partial q_r}{\partial r} \right) - k_{sd}q_r \quad (45)$$

with the fluid and solid coupled by

$$C_s = \left(\frac{q_r}{K_F} \right)^{\frac{1}{n_F}} \quad \text{at } r = R \quad (46)$$

where the boundary conditions are

$$\left. \frac{\partial q_r}{\partial r} \right|_{r=R} = \frac{k_f}{D_s \rho} (C - C_s) \quad (47)$$

$$\left. \frac{\partial q_r}{\partial r} \right|_{r=0} = 0 \quad (48)$$

and for the initial conditions

$$C(t, x = 0) = C_0 \quad (49)$$

Solution of the dual-resistance sorption model form of the ADR equation is somewhat more complex than the local-equilibrium model and the two-site model, but straightforward in concept. The macroscopic ADR equation (Equation 44) is solved simultaneously with a partial differential equation for the solid-phase for each spatial location in the discretized domain. The numerical method used to approximate this solution was constructed by using the finite difference method to reduce the set of partial differential equations to a

set of ordinary differential equations in time. A FORTRAN code was developed to solve the coupled set of ordinary differential equations simultaneously using Gear's algorithm (1971). Additional details of this numerical approximation approach are presented in Appendix III. Validation was accomplished by comparison with an available analytical solution (Rasmuson and Neretnieks, 1980; Miller and Weber, 1988).

RESULTS

BOTTLE-POINT EQUILIBRIUM EXPERIMENTAL RESULTS

The sorption equilibrium characteristics of the solutes p-dichlorobenzene and o-xylene and the Camp Lejeune subsurface solid were analyzed using the experimental procedures detailed in the Materials and Methods section. The experimental work with these materials proved to be extremely difficult because of the small amount of sorption that occurred.

It is good experimental design to plan bottle-point sorption experiments that result in a 50–80% decrease in the initial fluid-phase concentration. This is done to limit the error introduced by sorption to laboratory glassware, variation in extraction volumes, differential volatilization among samples, and gas chromatography response variations. To accomplish the desired reduction, the mass of solids to mass of solution ratio (or solids ratio) is manipulated. That is, the solids ratio is increased for poorly-sorbing solute-solid mixtures. The practical upper limit of the solids ratio is a function of the settling and compaction characteristics of the solid material but usually ranges from 1–2. As a benchmark, the solids ratio for an aquifer usually ranges from 3–5, or somewhat higher than that possible using bottle-point methods.

Sorption equilibrium studies with p-dichlorobenzene and o-xylene resulted in only about a 15% decrease in the fluid-phase concentration for the maximum solids concentration possible. As expected, the results from these experiments showed substantial experimental variation—resulting from the experimental problems noted above. Equilibrium isotherm plots for o-xylene and p-dichlorobenzene are shown by Figures 4 and 5.

The sorption-equilibrium models outlined in the Modeling section were fit to the data sets shown in Figures 4 and 5, by selecting model parameters that minimized the sum of squares of the relative error between model predictions and experimental data. This may be shown in equation form as

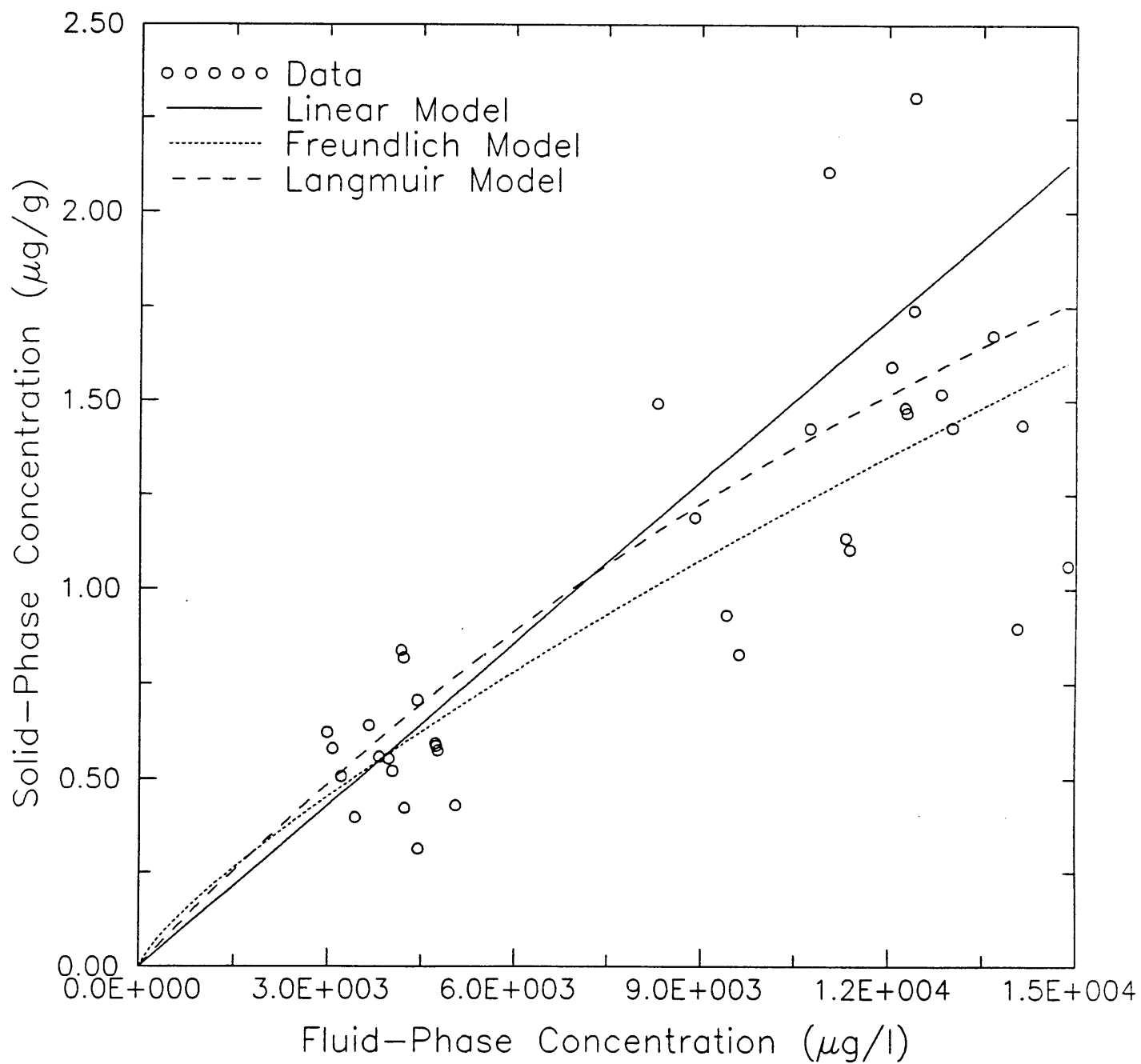


Figure 4. Sorption equilibrium data and model fits for the solute p-dichlorobenzene and the Camp Lejeune subsurface solid material.

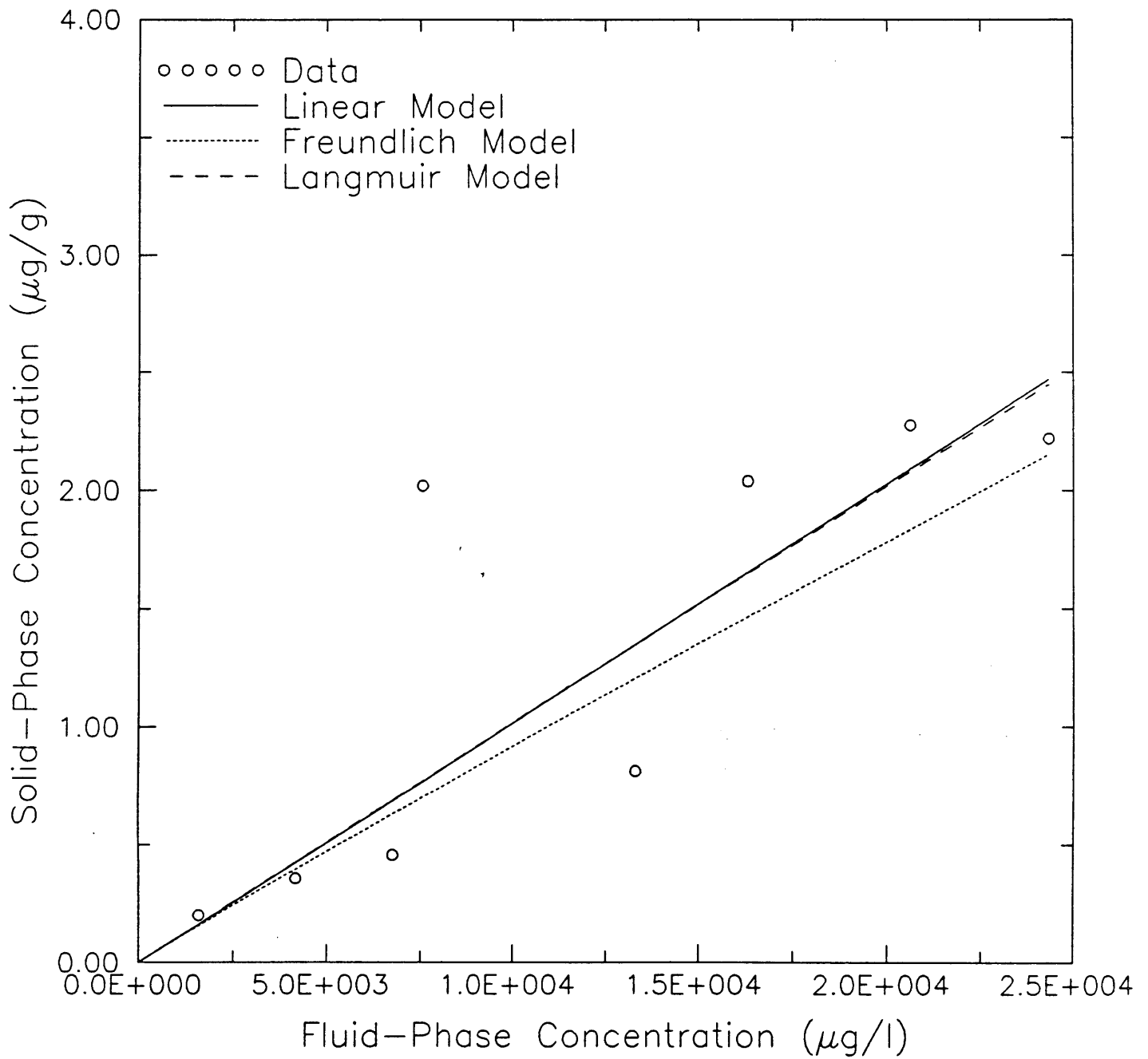


Figure 5. Sorption equilibrium data and model fits for the solute o-xylene and the Camp Lejeune subsurface solid material.

$$\min \varepsilon = \sum_i^{n_d} \left(\frac{q_{di} - q_{mi}}{q_{mi}} \right)^2 \quad (50)$$

where: i is a data-point index; n_d is the number of experimental data points, q_d is the experimental mass-average solid-phase solute concentration; and q_m is the model-predicted mass-average solid-phase solute concentration.

The results of the model fits are given in Table 3, while the best-fit model traces are overlain on the data plots given in Figures 4 and 5. The Freundlich model provided the best fit in both cases with typical values of n_F found, although practically and statistically all models yielded a similar agreement with the data. The mean error for the Freundlich model was 23.1% for p-dichlorobenzene and 24.1% for o-xylene solute. The error between these experimental data and the model fits is higher than the error normally achieved using similar procedures for more strongly sorbing solute-solid combinations.

Table 3. Sorption Equilibrium Parameter Summary

Model	Parameter	p-Dichlorobenzene		o-Xylene*	
		Value	Mean Error	Value	Mean Error
Linear	K_p (cm ³ /g)	1.43×10^{-1}	30.9%	1.01×10^{-1}	27.4%
Freundlich	K_F ((cm ³ /g) ^{n_F})	1.03×10^{-2}	23.1%	5.74×10^{-2}	24.1%
	n_F (cm ³ /g)	7.89×10^{-1}		9.59×10^{-1}	
Langmuir	Q° (g/g)	5.18×10^{-6}	26.7%	1.40×10^{-4}	27.4%
	b (cm ³ /g)	$3.45 \times 10^{+4}$		$7.30 \times 10^{+2}$	

* All computations performed neglected data outlier at $C_e=7,570 \mu\text{g/l}$

BOTTLE-POINT RATE EXPERIMENTAL RESULTS

The previously-noted experimental difficulties found with measuring equilibrium sorption were evident as well in the rate studies. This follows from the rate-study procedure,

which attempts to measure a trend in fluid-phase concentrations as a function of time. Problems were encountered with the equilibrium experiments because the total change in fluid-phase concentration was small compared to the potential sources of error. Thus, attempting to discern a trend as a function of time is a second-order effect that is even more prone to error. This is so because, the changes in concentration between two different times is a fraction of the total change in fluid-phase concentration.

The rate at which sorption occurs was analyzed for the solutes p-dichlorobenzene and o-xylene and the Camp Lejeune subsurface material, using the experimental procedures outlined in the Methods section. The results of these experiments are shown by Figure 6. The experimental conditions of these two rate studies are summarized in Table 4. The smaller reduction in fluid-phase concentration with the o-xylene solute compared to the p-dichlorobenzene solute is consistent with the slightly higher solids ratio used with the p-dichlorobenzene rate study and the respective octanol:water partition coefficients of the two solutes.

Table 4. Sorption Rate Study Conditions and Parameter Summary

Parameter	p-Dichlorobenzene	o-Xylene
Initial Concentration (mg/l)	8.20×10^0	1.64×10^1
Mass of Solid (g)	4.40×10^1	3.00×10^1
Volume of Solution (cm ³)	2.19×10^1	2.00×10^1
α (1/hr)	1.22×10^{-2}	—
Variance	8.05×10^{-4}	—
D_s (cm ² /hr)	1.16×10^{-6}	—
Variance	1.24×10^{-3}	—

The p-dichlorobenzene data set was used as input into the two-site and dual-resistance

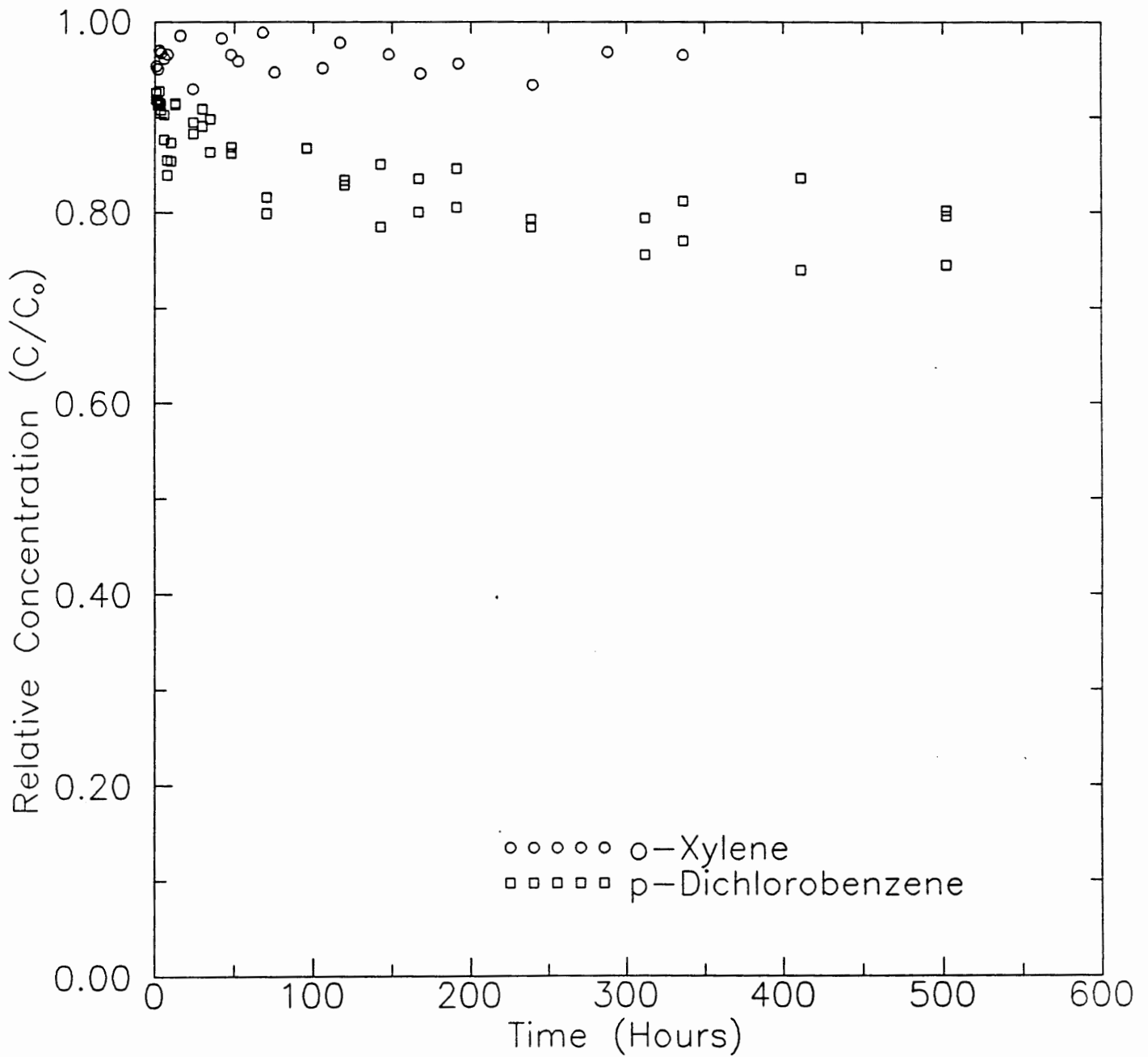


Figure 6. Batch reactor sorption-rate data for the Camp Lejeune subsurface solid material.

batch-reactor models presented in the Modeling section. Parameter estimation was performed using the objective function of minimization of variance between the observed and model-predicted concentrations. One parameter was estimated with each model: α for the two-site model, and D_s for the dual-resistance model. All other model inputs were independently determined. The Freundlich sorption-equilibrium model was used, with parameters determined from the bottle-point equilibrium study performed. The results of model fitting are graphically shown by Figure 7, while the rate parameters determined are given in Table 4.

The results of the sorption rate modeling of the p-dichlorobenzene solute are quite satisfying in view of the experimental uncertainties. Computed model variance was similar to published results for more ideal experimental conditions (Weber and Miller, 1988). Close inspection of the modeling results shows the traits of each model.

The two-site model predicts early response quite accurately, while predicting equilibrium conditions in less time than is actually required. This is a result of directly computing the fast-site component of sorption data from an experimental measurement made after one hour. This virtually assures good agreement with the experimental data during early times, and the approach of the two-site model toward equilibrium results from the minimization procedure used on the later data. Previous work (Weber and Miller, 1988) has shown this method to yield results that are in good agreement with parameter estimation methods based on adjusting two model parameters.

The best fit of the dual-resistance model shows a smooth descent from the initial concentration toward the eventual equilibrium. The shape of the model prediction is based entirely on a minimization of variance, and no particular portion of the data is assured a more accurate fit. Thus the character of the two rate model fits are somewhat different, although both provide a reasonably-accurate description of the observed response.

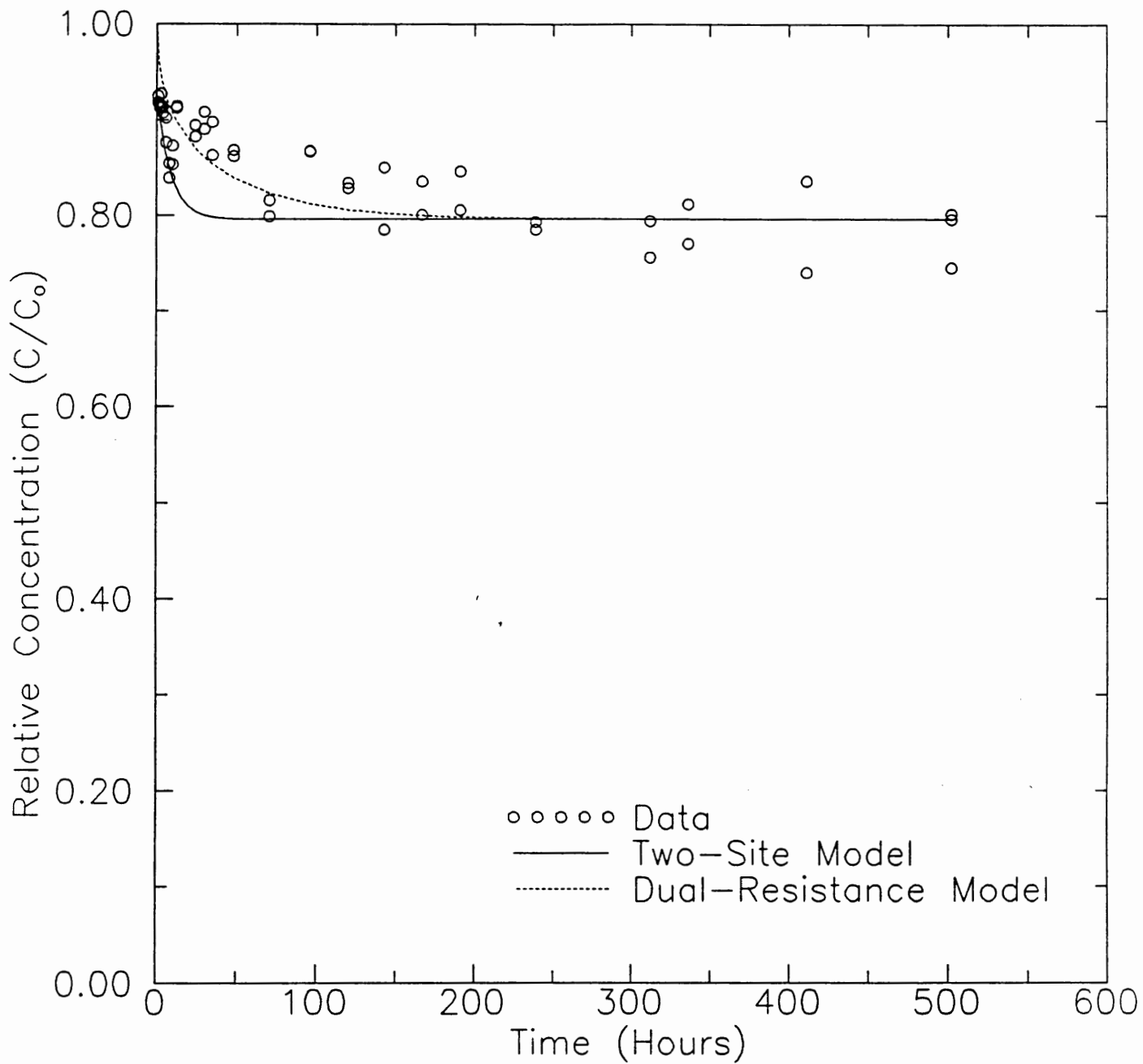


Figure 7. Batch-reactor rate model fits to experimental data for the solute p-dichlorobenzene and the Camp Lejeune subsurface solid material.

COLUMN-REACTOR EXPERIMENTAL RESULTS

The column experimental apparatus discussed in the Materials and Methods section was used to investigate the movement of a nonreactive chloride and sodium azide solute, and the movement of a toluene and o-xylene solute. The investigative methodology required the analysis of the data for nonreactive solute profiles resulting from a step source of contaminant to determine the spreading of a solute front caused by hydrodynamic dispersion. These data were collected by supplying a known and constant concentration of a nonreactive solute in a column and observing the change in concentration in the effluent of the column. The results of such an analytical procedure are shown on Figure 8.

Also shown on Figure 8 are the relevant characteristics of the column, the advective-dispersive model fit value for hydrodynamic dispersion, and a trace of the modeled concentration as a function of time. Parameter estimation was accomplished using a Levenberg-Marquardt algorithm defined to minimize the variance between the observed and predicted normalized concentrations. The results of this model analysis agree well with the data collected, and the front observed in the column used is quite sharp. That is, the relative concentration of the effluent of the column changes abruptly from near zero at 0.80 bed volumes (or theoretical retention times) to near unity at 1.20 bed volumes. This gives a Peclet number ($P_e = v_x X / D_x$) of 469 for the column system, which is considered rather sharp. Sharp fronts like the ones shown in Figure 8 can make the accurate modeling of contaminant transport using an ADR-equation approach rather expensive.

The column apparatus was also used to observe the movement of the target compounds toluene and o-xylene through the system. Figure 9 shows the effluent concentration for the target solutes as a function of bed volumes. A step source (slightly declining in time due to volatilization) of the organic solutes was fed to the column for 1,710 minutes or about 2.25 bed volumes, while observations of organic solute concentrations were made for the column effluent for a total time equivalent to 9.05 bed volumes. It may be observed that the organic solute data showed a similar sharp front to the nonreactive tracer data and

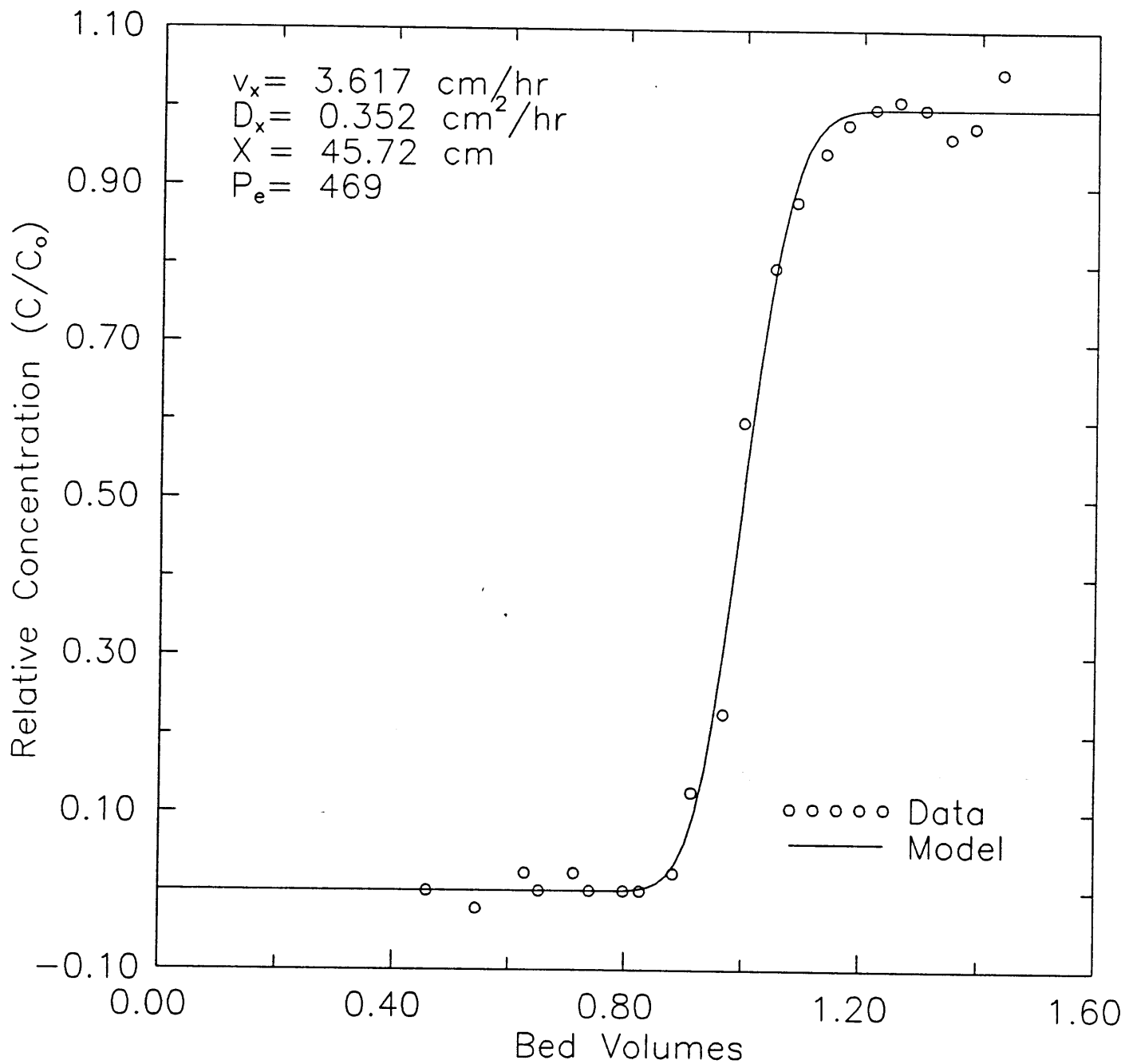


Figure 8. Column tracer data and nonreactive advective-dispersive model fit.

also exited at about one bed volume. This is an indication that relatively little sorption occurred of the organic solutes to the Camp Lejeune solid material. This is consistent with the findings from the bottle-point studies.

The *o*-xylene data shown in Figure 9 were evaluated using four models: a nonreactive model, which assumed no sorption occurred; a linear local equilibrium model; a nonlinear local equilibrium model; and a two-site model. Each of these models was applied in a predictive mode—using estimates of parameters available from the bottle-point experiments. This approach wasn't directly possible for the two-site model, since rate experimental results from the bottle-point rate study were not suitable for parameter estimation. Therefore, for the two-site model α for *o*-xylene was assumed equivalent to α for *p*-dichlorobenzene. The ratio between fast and slow sorption was also assumed to be equivalent for *o*-xylene and *p*-dichlorobenzene. These assumptions are reasonable based on previously-published results (Weber and Miller, 1988; Miller and Weber, 1988). A column simulation parameter summary is given in Table 5, while the results of the model predictions are given in Figure 10.

The modeling results show that some sorption did occur, because the nonreactive model predicted both the solute front and elution front would occur earlier in time than was experimentally found. The linear equilibrium model and the nonlinear equilibrium model showed similar fits to the data—deviating from the data for the sorption portion of the data but closely approximating the desorption portion of the data. The similar fit for the two equilibrium approaches is expected because of the small deviation from linearity for the *o*-xylene solute. The best fit to the sorption portion of the data was given by the two-site model. It may also be observed that the two-site model predicted a long tail on the desorption portion of the model simulation. It is clear that the data showed more of a tail than was predicted by the equilibrium models. It isn't clear exactly how long the elution tail persisted, because of the low sensitivity of measuring small concentrations of *o*-xylene using gas chromatography procedures.

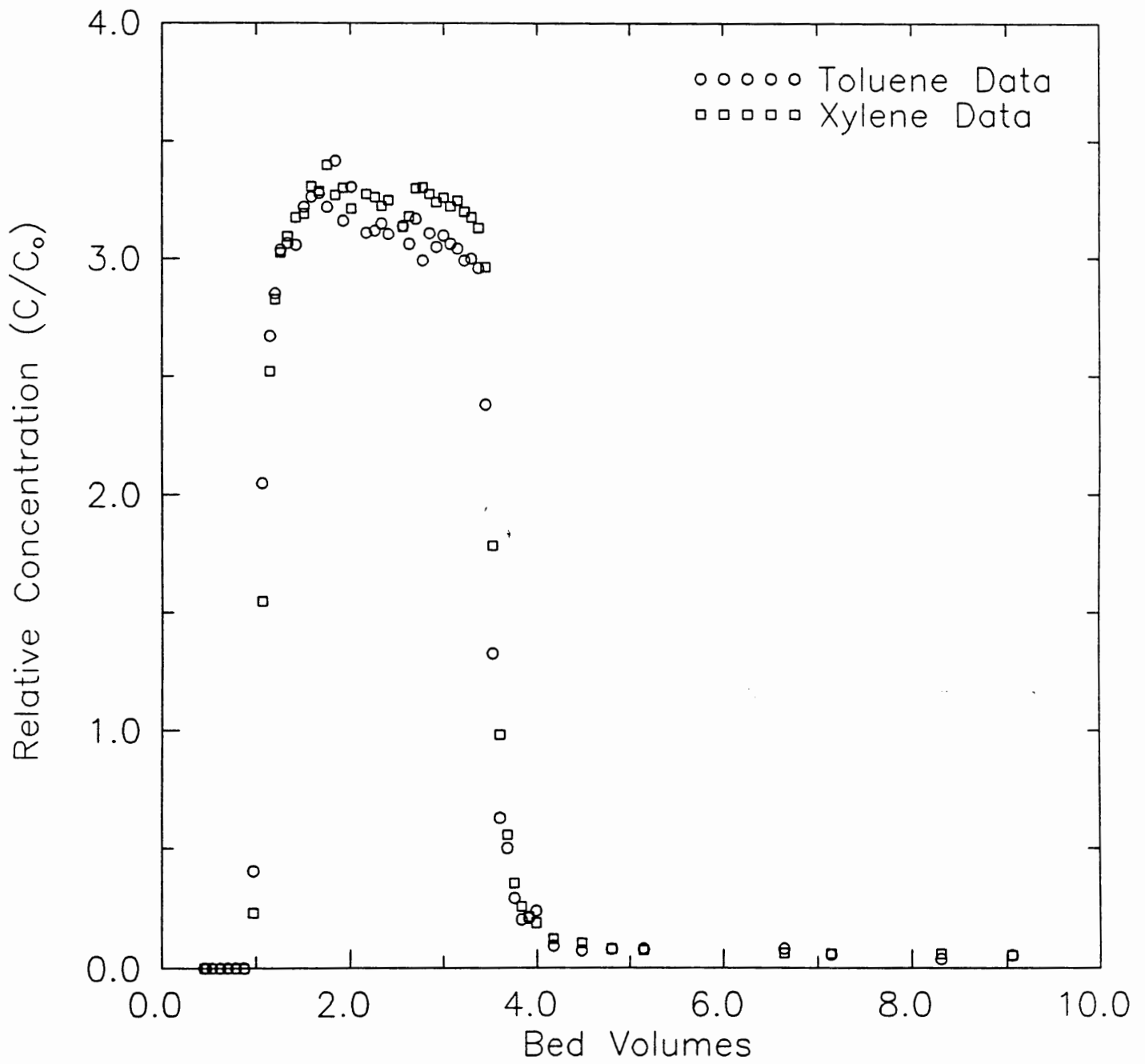


Figure 9. Column data for organic solutes.

Table 5. Column Simulation Parameter Summary for o-Xylene

Model	Parameter	Value	Units
Nonreactive	ρ	2.64×10^0	g/cm^3
	X	4.57×10^1	cm
	n	4.08×10^{-1}	
	v_x	3.62×10^0	cm/hr
	D_x	3.52×10^{-1}	cm^2/hr
Linear Equilibrium	K_p	1.01×10^{-1}	cm^3/g
Nonlinear Equilibrium	K_F	5.74×10^{-2}	$(\text{cm}^3/\text{g})^{n_F}$
	n_F	9.59×10^{-1}	
Two-Site	K_f	1.86×10^{-2}	$(\text{cm}^3/\text{g})^{n_f}$
	K_s	3.88×10^{-2}	$(\text{cm}^3/\text{g})^{n_s}$
	n_f	9.59×10^{-1}	
	n_s	9.59×10^{-1}	
	α	1.22×10^{-2}	1/hr

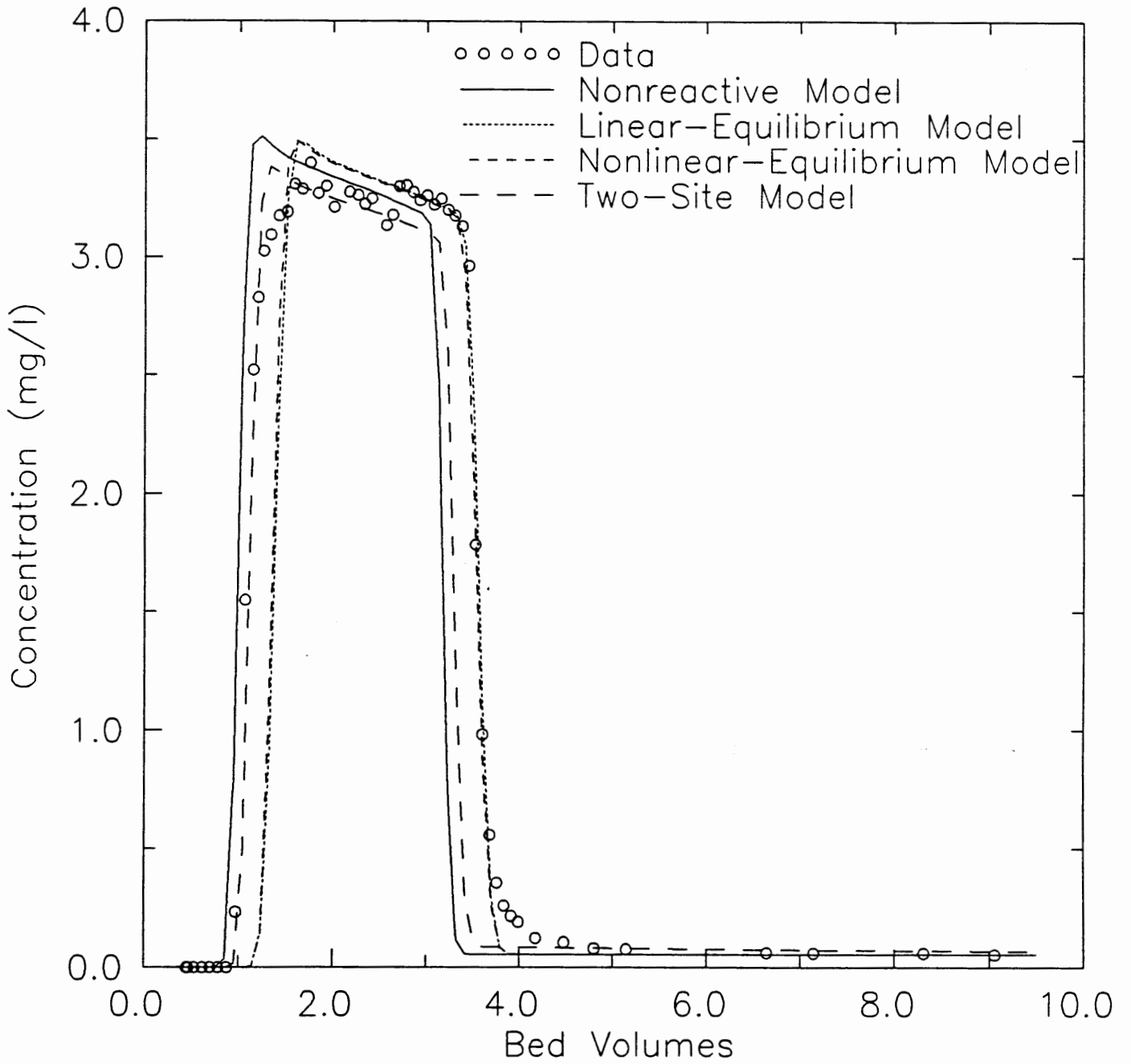


Figure 10. Column data for o-xylene and model predictions.

DISCUSSION

GENERAL

The results of the experimental work performed show that only a small amount of sorption of moderately hydrophobic solutes occurred to the Camp Lejeune subsurface material. Since only a small amount of sorption occurred, the effect of the rate of sorption on solute movement and aquifer rehabilitation was difficult to precisely determine experimentally. However, the data collected did clearly show that: sorption was not instantaneous; a two-site sorption rate model provided a better description of the sorption data collected than an equilibrium-based approach; and the two-site rate model predicted, and the experimental data showed, a long tail for the elution of o-xylene from a column experiment. The existence of this long tail in both model predictions and experimental data confirms the original hypothesis of the research that sorption and desorption effects contribute to increased aquifer clean-up times.

The effect on the clean-up time for a given aquifer is a function of the contaminant source distribution, the solute of concern, the solid-phase properties, and the clean-up level needed for the given solute. That is, a long tail is not important if the concentration is less than the clean-up target concentration for the intended use of the aquifer. For many contamination incidents, the clean-up level is a drinking water standard, and drinking water standards are becoming increasingly more stringent. This suggests that the effect of the sorption/desorption processes on the time required for aquifer restoration will become more important as water quality standards become more stringent.

The implications of the research findings to the coastal region of North Carolina are clear:

1. Sorption of moderately hydrophobic organic solutes to subsurface material has only a slight effect on movement of an advancing contaminant front—assuming that the Camp Lejeune material investigated is typical of coastal subsurface material;

2. Sorption equilibrium and rate parameters determined for o-xylene and p-dichlorobenzene to Camp Lejeune subsurface material were consistent with parameters found for other natural materials that are low in organic carbon; and
3. The real significance of the sorption rate effect is a function of the solute and solid properties and the contaminant action level of the aquifer rehabilitation.

The results of this research may be examined in greater detail and generalized with respect to several considerations:

1. constitutive approximations of sorption equilibrium;
2. effect of hydrodynamics on aquifer remediation;
3. effect of sorption equilibrium on aquifer remediation; and
4. the effect of sorption rate on aquifer remediation.

The subsections that follow examine these considerations.

CONSTITUTIVE APPROXIMATIONS OF SORPTION EQUILIBRIUM

The experimental methods used to measure sorption equilibrium in this work are straightforward. However, these measurements are time consuming to perform and require skill and diligence by the analyst for accurate results. For this reason, it is desirable to have an empirical method for making a first-cut estimate of sorption equilibrium without performing time-consuming experiments. Many such methods have been proposed during the last decade, which are based on the properties of the solute and solid material.

In one of the first and most comprehensive studies, Karickhoff et al. (1979) investigated sorption of a variety of neutral, nonpolar, hydrophobic, organic compounds on sediments and reported the relationship

$$\log K_{oc} = \log K_{ow} - 0.21 \quad (51)$$

for

$$K_p = f_{oc}K_{oc} \quad (52)$$

in which K_{oc} is the organic carbon normalized partition coefficient of the solid, K_{ow} is the octanol-water partition coefficient of the solute, and f_{oc} is the mass fraction of organic carbon in the solid material. Octanol-water partition coefficients are readily available in the literature for a wide variety of compounds (Hansch and Leo, 1979).

In a recent study, Sabljic (1987) reviewed a variety of empirical methods for predicting sorption equilibrium between organic solutes and natural solid materials. Sabljic (1987) found that a method based on the molecular connectivity index of the solute and the organic carbon mass fraction of the solid material gave the best level of prediction for a wide range of experimental data. Molecular connectivity (χ) is a topological method that is a measure of the projected size of a molecule, and χ is computed using only the molecular structure bond information. Sabljic also presented extensions to the molecular connectivity method that allow for accurate predictions of sorption equilibrium for polar solutes. The principal advantage of this method results from the definite nature of a computed value of χ compared to experimentally-determined properties such as octanol:water partition coefficient or aqueous solubility.

Table 6 shows a comparison of observed and predicted organic-carbon-normalized partition coefficients for the solutes p-dichlorobenzene and o-xylene. For the laboratory measurements made in the experimental portion of this investigation, the molecular topology model of Sabljic (1987) provided a better approximation than the popular Karickhoff et al. (1979) model. The mean error for the Karickhoff model prediction was 127%, while the mean error for the Sabljic model was 28%. It should be observed that both of these approximations are within the normal range expected for constitutive approximations of sorption, which is a factor of 2-3.

The Karickhoff relationship tended to predict larger values of K_{oc} than were noted,

while the molecular topology method of Sabljic under-predicted the measured values of K_{oc} . This lends even further confidence in the Sabljic molecular topology method since the organic carbon fraction in the Camp Lejeune material was extremely low and mineral site sorption may account for a significant fraction of the total sorption. Since K_{oc} is an organic-carbon-normalized partition coefficient, the effect of sorption to mineral sites is ignored, and it is expected that sorption estimation methods that ignore mineral sorption would under-predict the actual sorption observed in a low-carbon system.

Table 6. Observed and Predicted Linear Partition Coefficients

Source	p-Dichlorobenzene	o-Xylene
Measured K_{oc}	596	423
Predicted K_{oc} (Karickhoff et al., 1979)	1479	871
Predicted K_{oc} (Sabljic, 1987)	353	360

It should be noted that the above comparisons are based upon empirical estimates of sorption, and they do not take the place of actual measurements of the relationship. This is so not only because the estimates are subject to an error due to the exact nature of the solid and solute, but also because sorption equilibrium relationships are typically nonlinear when observed over a wide range in equilibrium concentration (Hamaker and Thompson, 1972; Weber and Miller, 1989). Nonlinearity of the sorption equilibrium relationship was also found for the materials investigated in this work. The importance of this point for aquifer restoration will be investigated further.

EFFECT OF HYDRODYNAMICS ON AQUIFER REMEDIATION

Several factors affect the time required to renovate a contaminated aquifer. The hy-

hydrodynamic processes of advection and dispersion are chief concerns in assessing the time required to renovate an aquifer. While a complete discussion of hydrodynamic processes will not be presented herein, two major points will be made: (1) dimensionless-form equations can be derived to aid in showing how clean-up times increase as a function of increased system dispersion; and (2) subsurface heterogeneity leads to hydrodynamic conditions that result in increased clean-up times when compared to homogeneous conditions.

Consider the case of the one-dimensional ADR equation that includes linear local-equilibrium sorption with first-order decay from the fluid and solid phase

$$R_f \frac{\partial C}{\partial t} = D_x \frac{\partial^2 C}{\partial x^2} - v_x \frac{\partial C}{\partial x} - k_{fd}C - \frac{\rho_b k_{sd} K_p}{n} C \quad (53)$$

defining the variable groupings

$$\tau = \frac{X}{v_x} \quad (54)$$

$$P_e = \frac{v_x X}{D_x} \quad (55)$$

$$k_e = k_{fd} + \frac{\rho_b k_{sd} K_p}{n} \quad (56)$$

$$\bar{t} = \frac{t}{R_f \tau} \quad (57)$$

$$\bar{C} = \frac{C}{C_o} \quad (58)$$

$$\bar{x} = \frac{x}{X} \quad (59)$$

$$\bar{k}_e = \tau k_e \quad (60)$$

where: X is a spatial reference location; τ is the average advective travel time to X ; P_e is a dimensionless Peclet number; k_e is an effective first-order decay rate; \bar{t} is a dimensionless variable in time termed throughput; \bar{C} is dimensionless concentration; \bar{x} is dimensionless distance; and \bar{k}_e is a dimensionless effective decay rate.

Equation 53 can be written in dimensionless form using equations 54 to 60 giving

$$\frac{\partial \bar{C}}{\partial \bar{t}} = \frac{1}{P_e} \frac{\partial^2 \bar{C}}{\partial \bar{x}^2} - \frac{\partial \bar{C}}{\partial \bar{x}} - \bar{k}_e \bar{C} \quad (61)$$

It follows from equation 61 that if dimensionless concentration is expressed as a function of throughput, the only variables that effect the shape of the resulting distribution are P_e and \bar{k}_e . In the absence of decay reactions, the P_e is the sole master variable. Figure 11 shows distributions of normalized concentration (\bar{C}) as a function of throughput (\bar{t}) for a range of P_e . The source condition used in Figure 11 was a step source that continued for a length of time equivalent to $\bar{t} = 3$.

Figure 11 shows that as P_e decreases the value of \bar{t} required for an approach of \bar{C} to 0 increases. This translates to longer cleanup times for higher dispersivity—making dispersion an important component in assessing the length of time required for aquifer renovation.

However, recent work has shown that dispersivities tend to be rather small when heterogeneity—especially in the vertical dimension—is considered (Molz et al., 1987), and even relatively homogeneous aquifers have been found to have wide ranges of hydraulic conductivity (Sudicky, 1986). Molz and co-workers found that field studies often report large values of dispersivities that are scale dependent, but these results are really manifestations of using vertically-averaged values of dispersivities in two-dimensional models that ignore heterogeneity. It seems clear that the fundamental pore-scale mechanisms that are normally associated with dispersion are a relatively small component of the dispersivity reported at the field scale. This suggests that when heterogeneity is considered true Peclet numbers become quite large, since D_x is usually small. Molz et al. (1987) report good agreement of model prediction and experimental data for field-scale tracer experiments, which were based on observed hydraulic conductivity variations and did not use dispersivity as a fitting parameter.

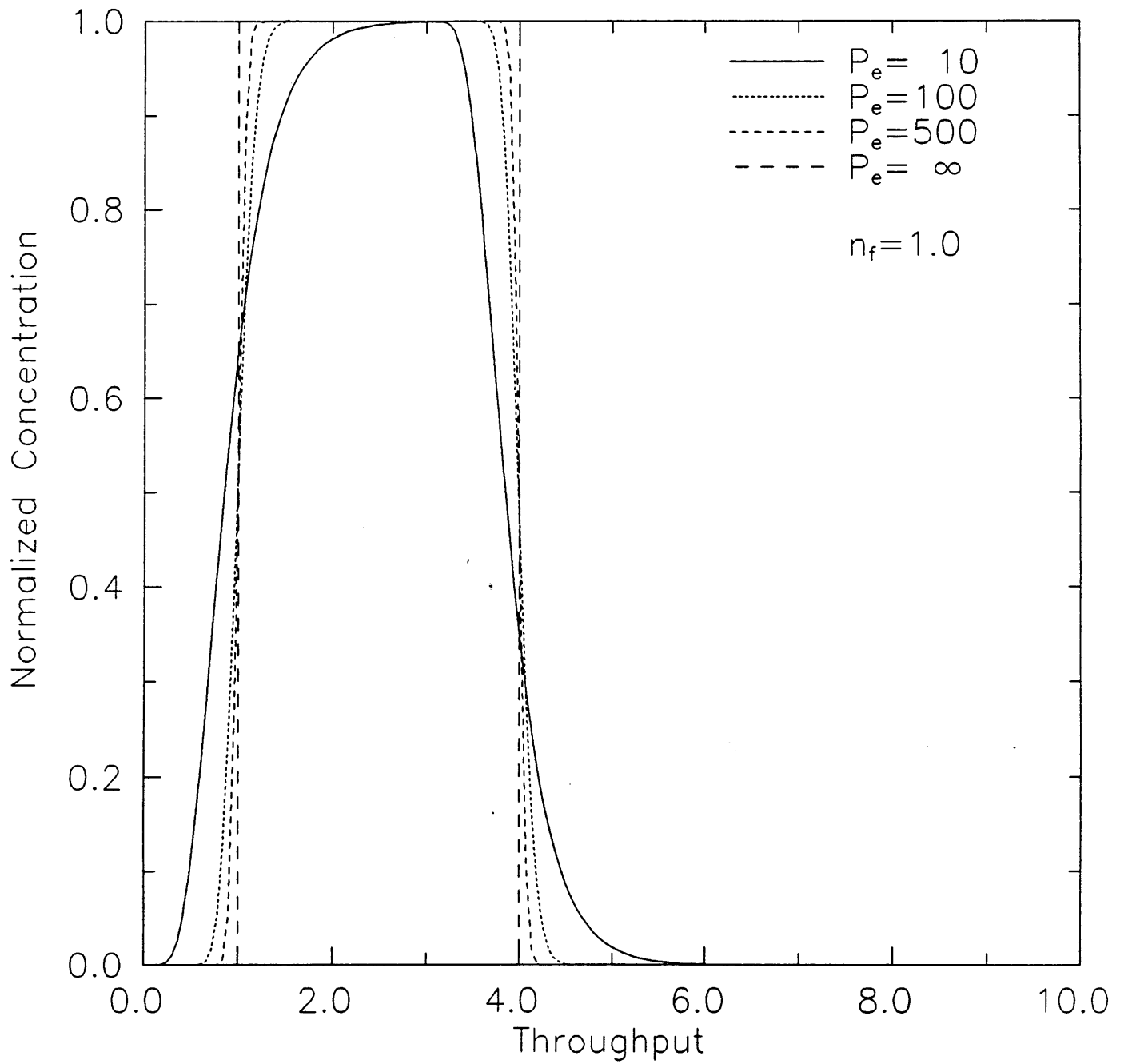


Figure 11. Dimensionless concentration profiles for linear, local-equilibrium sorption as a function of P_e .

The above discussion supports the conclusion that dispersion does not contribute significantly to the commonly-observed long cleanup times needed for aquifer restoration. System Peclet numbers can be expected to be large enough at the field scale that sharp-front solutions are reasonably accurate. This suggests that heterogeneity is a major factor affecting system hydrodynamics and hence cleanup time at the field scale.

A vertically-layered system with horizontal flow can be considered as an idealized heterogeneous system—this may be a good first-cut approximation for many aquifer systems. In a vertically-layered system, contaminants will move more rapidly through high conductivity regions. It follows that separate sharp fronts will develop in each layer, because of the velocity contrasts that exist between layers. This will be tempered somewhat by inter-layer transverse dispersion. It also follows that during aquifer remediation, high conductivity layers will be renovated more quickly than low conductivity layers because of differential velocity considerations. If a wide range of hydraulic conductivities exists, then the low velocity layers will give rise to a long tail on a vertically-averaged concentration profile as a function of time, at a purge well.

The greater the heterogeneity in the vertical direction the longer the concentration tail. The system tailing would be even longer if sorption equilibrium was inversely related to hydraulic conductivity, which would be the expected trend for many subsurface systems.

It is concluded that subsurface heterogeneity is the dominant hydrodynamic factor that leads to prolonged cleanup times. It is important to identify and quantify this heterogeneity if accurate estimates of contaminant movement and aquifer rehabilitation times are to be made. Much more remains to be done in field and analytical methods for assessing heterogeneity and routinely incorporating the effects into simulation models.

EFFECT OF SORPTION EQUILIBRIUM ON AQUIFER REMEDIATION

In addition to subsurface hydrodynamic heterogeneity, deviations from instantaneous linear-equilibrium sorption can also affect the time required for aquifer renovation. The

magnitude of this effect is a function of the degree of nonlinearity and the concentration level required for a given cleanup.

When equilibrium is nonlinear, the retardation factor becomes a function of concentration, hence time. The retardation factor for a Freundlich isotherm may be expressed as a function of an initial concentration C_i and a final concentration C_f

$$R_f = \frac{\int_{\bar{C}_i}^{\bar{C}_f} \left(1 + \frac{\rho_b q_o n_f \bar{C}^{n_f-1}}{n C_o}\right) d\bar{C}}{\bar{C}_f - \bar{C}_i} \quad (62)$$

where

$$\bar{C}_i = \frac{C_i}{C_o} \quad (63)$$

$$\bar{C}_f = \frac{C_f}{C_o} \quad (64)$$

$$q_o = K_f C_o^{n_f} \quad (65)$$

For the case where $C_i = 0$ and $C_f = 1$, equation 62 becomes

$$R_f = 1 + \frac{\rho_b q_o}{n C_o} \quad (66)$$

and

$$\bar{t} = \frac{t}{\tau \left(1 + \frac{\rho_b q_o}{n C_o}\right)} \quad (67)$$

Equation 66 will be used as a constant in presenting dimensionless analysis results for non-linear Freundlich-type equilibrium in the remainder of the Discussion in the form of \bar{t} given by equation 67. It is important to note that while results are presented in dimensionless form, they are still somewhat dependent upon actual system variables.

Figure 12 shows the resulting normalized concentration profiles from a step source of a duration of $\bar{t} = 3.0$, as a function of n_f . The results of this analysis show that as n_f decreases the length of the tail on the elution portion of the concentration profile increases. Therefore aquifer remediation time is inversely related to the value of the Freundlich exponent for desorption, where desorption is described by the Freundlich isotherm. A typical range of the Freundlich exponent for sorption is $0.7 \leq n_f \leq 1.0$ (Weber and Miller, 1989), however desorption has been observed to display hysteresis. Desorption hysteresis may lead to Freundlich desorption exponents as low as $n_f = 0.3$ (Swanson and Dutt, 1973).

The results presented in Figure 12 are re-plotted in Figure 13 in a form of $\log \bar{C}$ as a function of \bar{t} for a range of n_f . This is significant since drinking water quality standards often dictate cleanup levels, and these standards may be several orders of magnitude less than the maximum concentration existing in a system. Figure 13 shows that prolonged cleanup times would be the expected result from nonlinear sorption described by the Freundlich isotherm.

Long-term simulations were performed for the same conditions shown in Figures 12 and 13, but starting from the initial condition of $\bar{C}(\bar{t} = 0, \bar{x}) = 1$. The objective of these long-term simulations was to quantify the time required to reach action levels down to $\bar{C} = 10^{-6}$. The results of these long-term simulations are presented in Figure 14 and show the significance of this factor. The logarithm of cleanup time is linearly related to the value of the desorption exponent over the range shown by Figure 14. Cleanup times relative to linear equilibrium sorption to reach $\bar{C} = 10^{-6}$ would be expected to increase: by a factor of about 4 for mild nonlinearity ($n_f = 0.8$), and by a factor of about 420 for a solute that displays hysteresis typical with laboratory findings ($n_f = 0.4$). These results support the conclusion that nonlinearity of sorption/desorption equilibrium between a solute in solution and sorbed to a solid phase can have a profound effect on the length of time required to renovate an aquifer. The significance of this factor can be expected to increase as water quality standards become more stringent.

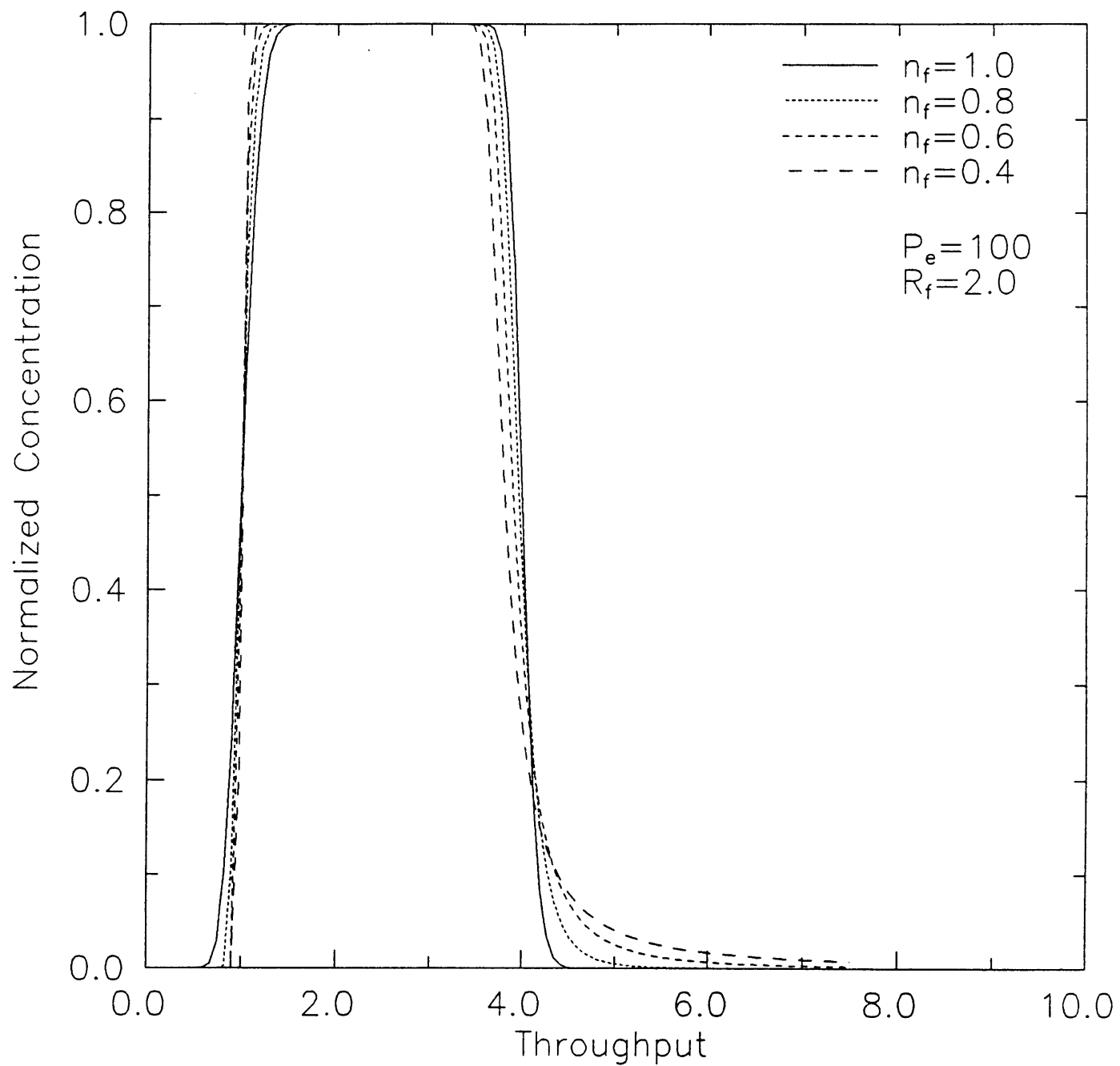


Figure 12. The effect of n_f on solute elution time for a step source of duration $\bar{t} = 3$.

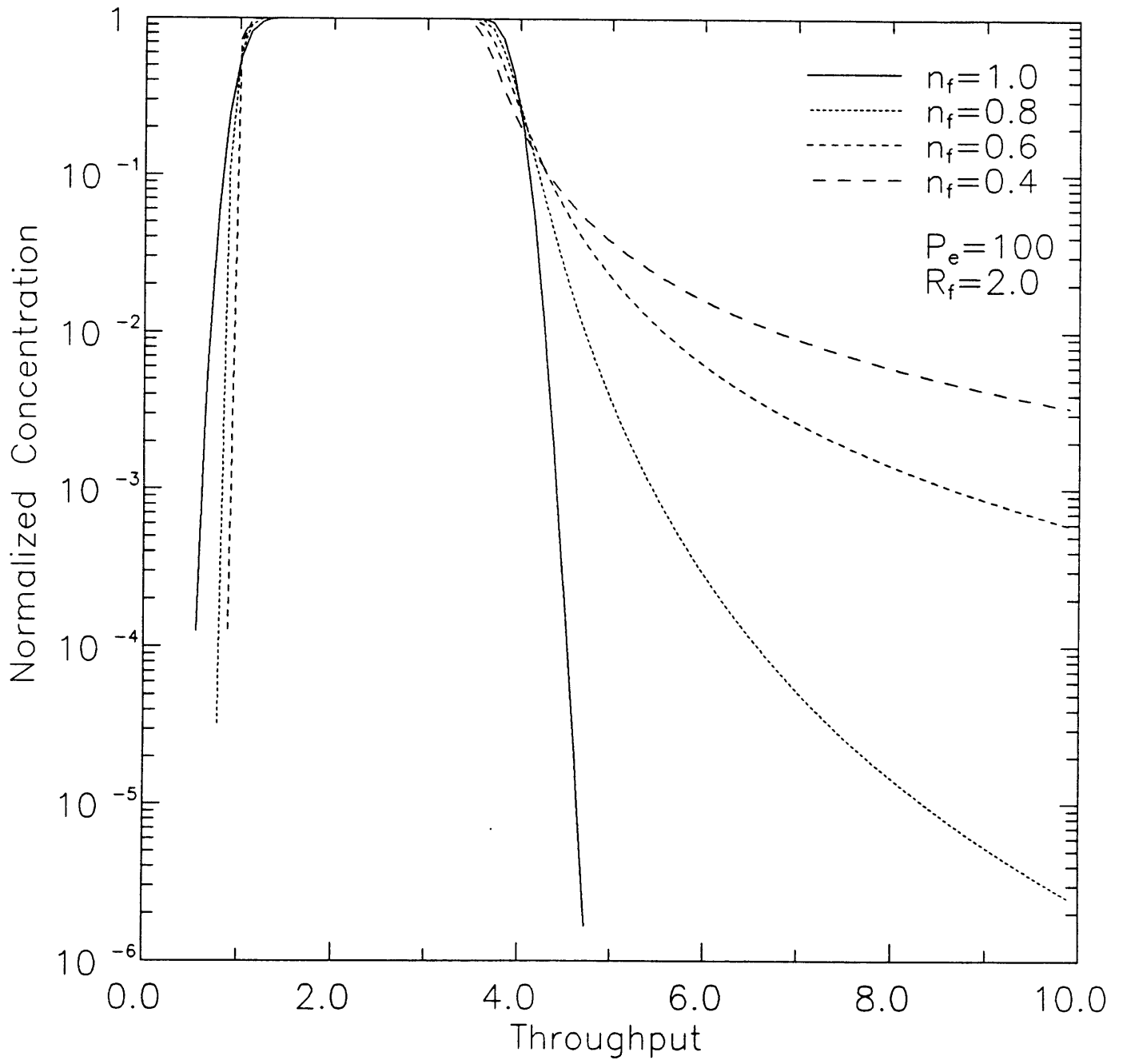


Figure 13. The effect of n_f on solute elution time for concentrations significantly less than the maximum system concentration.

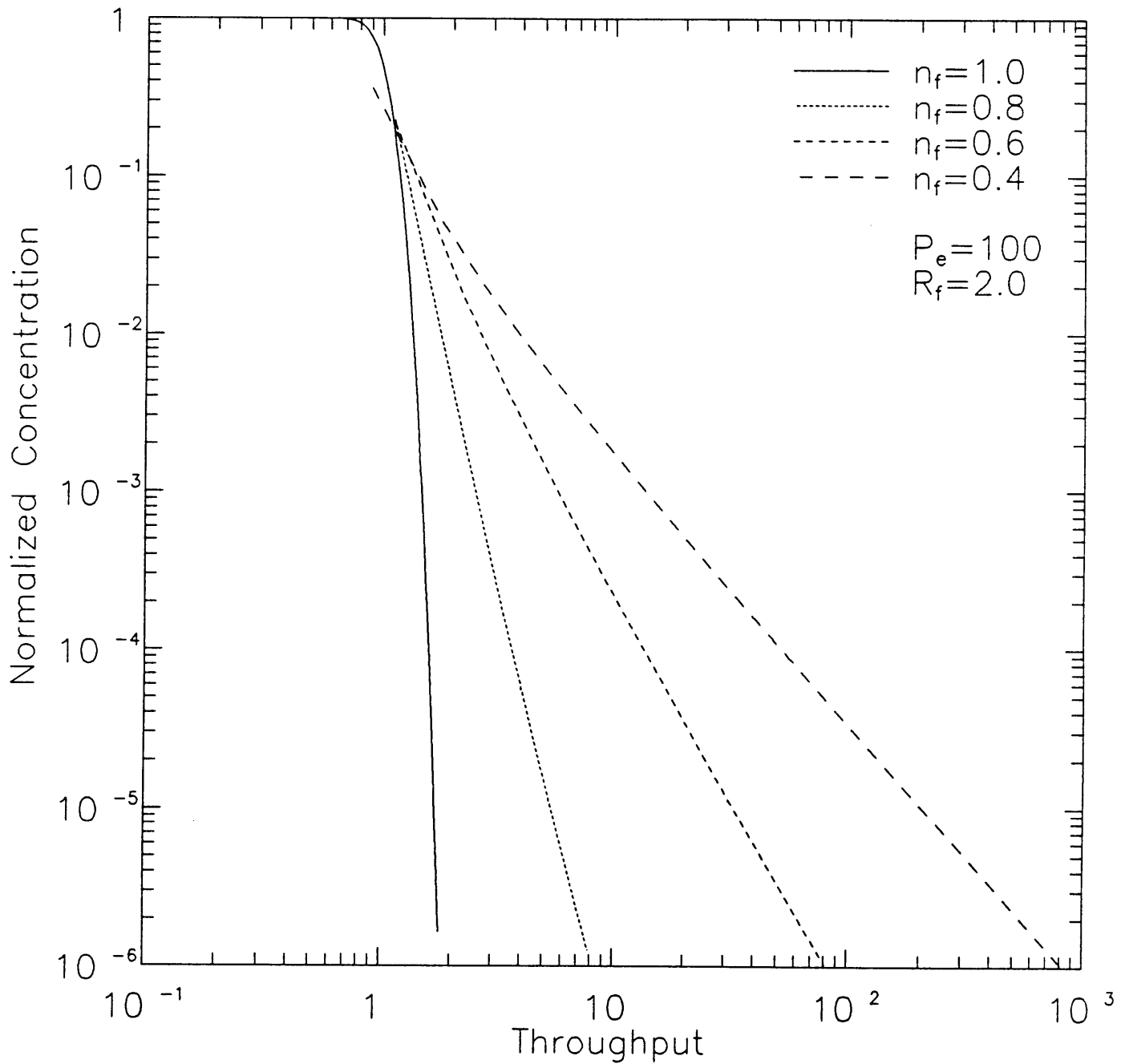


Figure 14. The effect of n_f on solute elution time required to reach low concentration action levels.

EFFECT OF SORPTION RATE ON AQUIFER REMEDIATION

The rate at which the sorption and desorption reaction occurs can also be expected to influence the movement of a solute mass and length of time required to renovate a contaminated aquifer. The two-site model form of the ADR equation may be used to investigate the effect of reaction rate on cleanup time. A dimensionless Damkohler number, D_a , is introduced to aid in describing the effects of sorption rate in general terms

$$D_a = \frac{\tau \rho_b q_o}{n C_o} \alpha \quad (68)$$

It should be noted that similar to the dimensionless analysis performed for nonlinear equilibrium, the results presented using the D_a described by equation 68 are dependent upon the actual input values of variables used in the ADR model. Other investigators have shown this dependency varies with the form of the dimensionless grouping used, but the variable effect is always present (Bahr and Rubin, 1987; Jennings, 1987). For this reason, the results presented in this section will be given for $R_f = 2.0$ and $R_f = 20.0$, and for $n_f = 1.0$ and $n_f = 0.8$.

Figures 15 to 18 show simulated normalized concentration profiles for four combinations of R_f and n_f , for a step source of duration $\bar{t} = 3$. Figures 15 to 18 show that the time required to cleanup an aquifer would be expected to increase as a function of decreasing D_a . It may also be observed that for increasing R_f a fixed D_a is somewhat farther away from an equilibrium condition. In all cases the largest D_a simulated gives results that are essentially identical to local equilibrium conditions, while values of $D_a < 1$ were not simulated but would certainly exist for transport on a small spatial scale with a slowly-sorbing solute.

The two conditions used to produce Figures 17 and Figure 18 were further investigated by performing elution simulations to simulate the time required to reach low concentrations from an initial condition of $\bar{C}(\bar{t} = 0, \bar{x}) = 1$. These results are presented in Figures 19 and

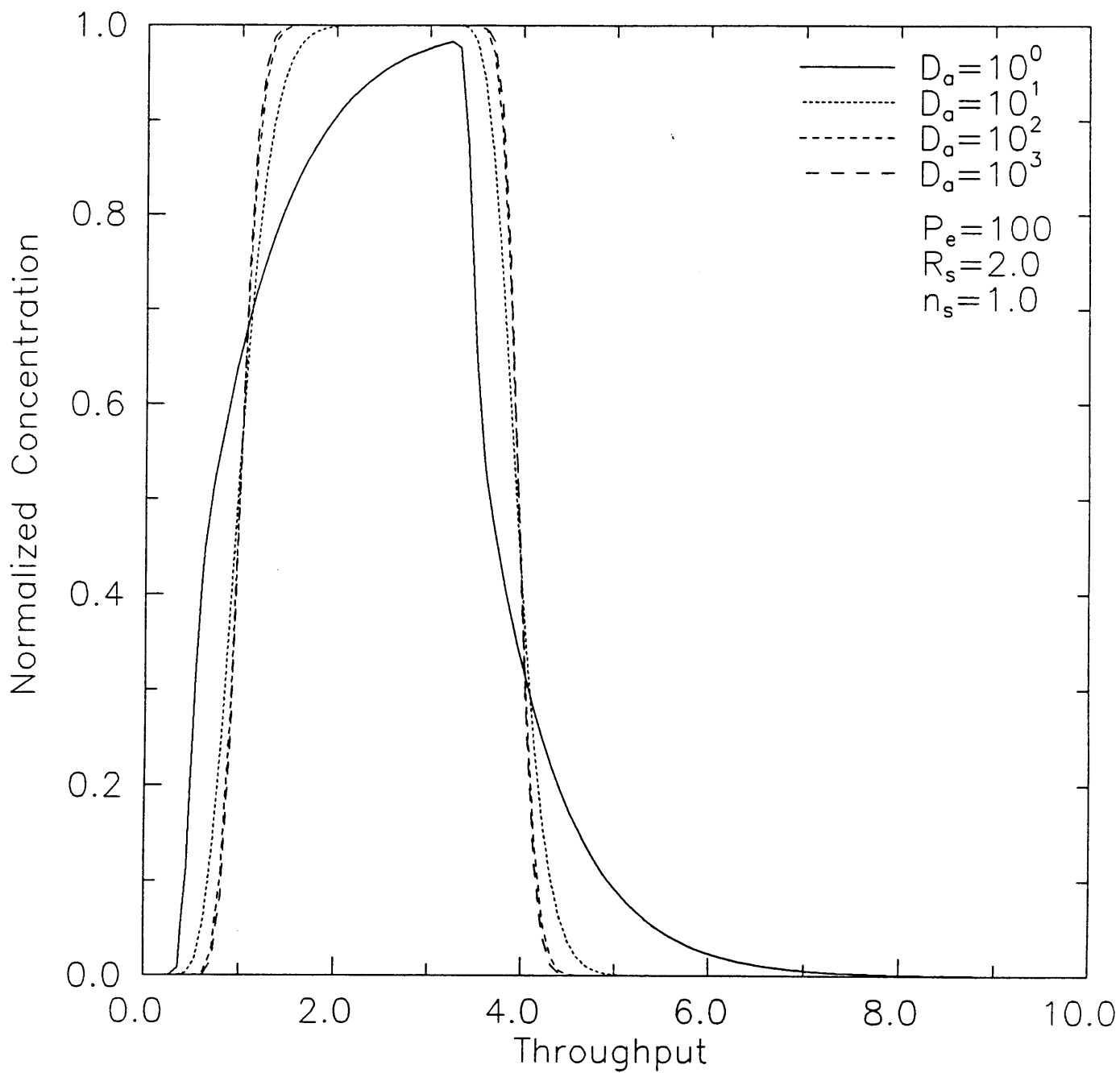


Figure 15. Normalized concentration profiles as a function of D_a for $R_f = 2.0$ and $n_f = 1.0$.

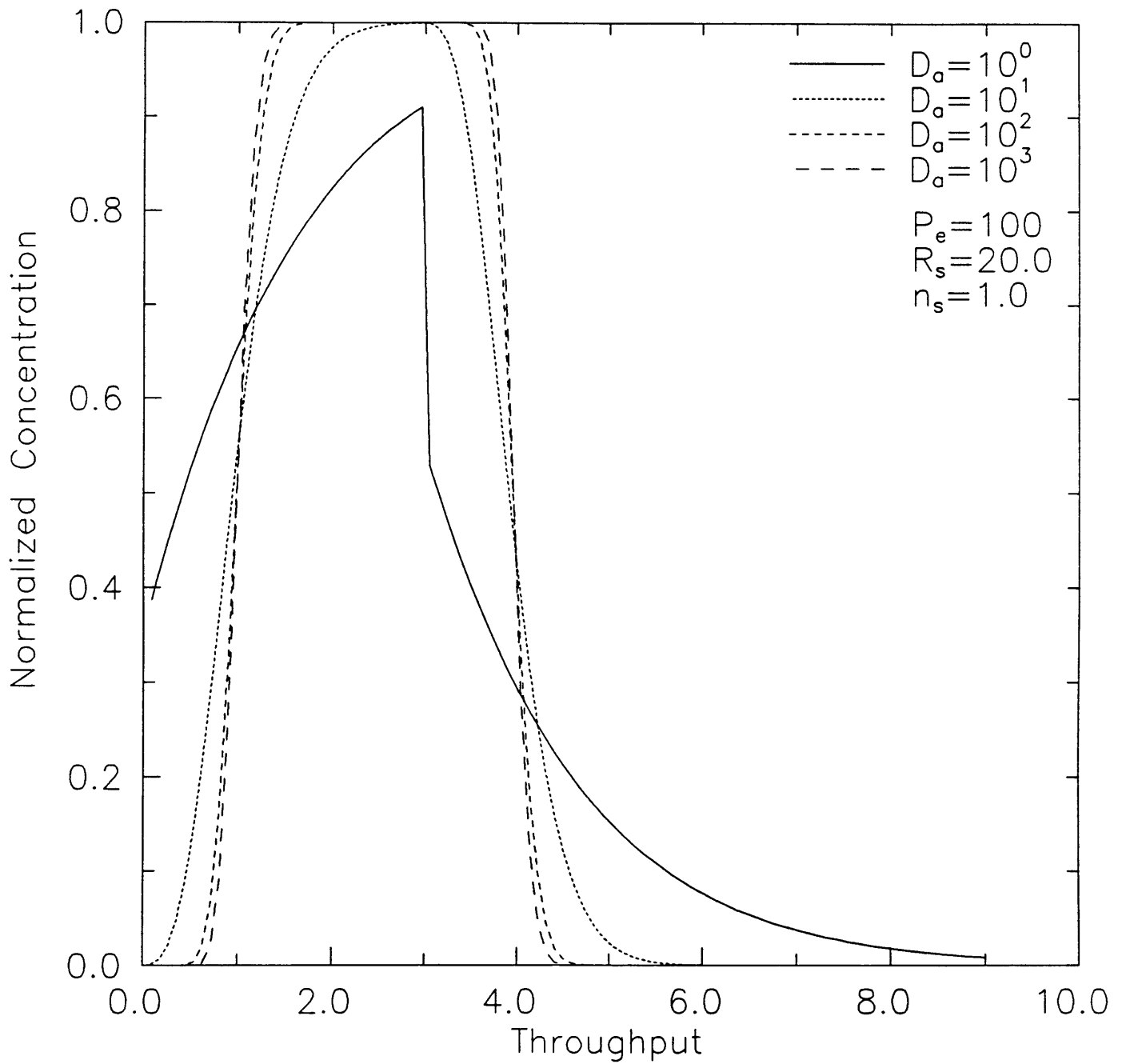


Figure 16. Normalized concentration profiles as a function of D_a for $R_f = 20.0$ and $n_f = 1.0$.

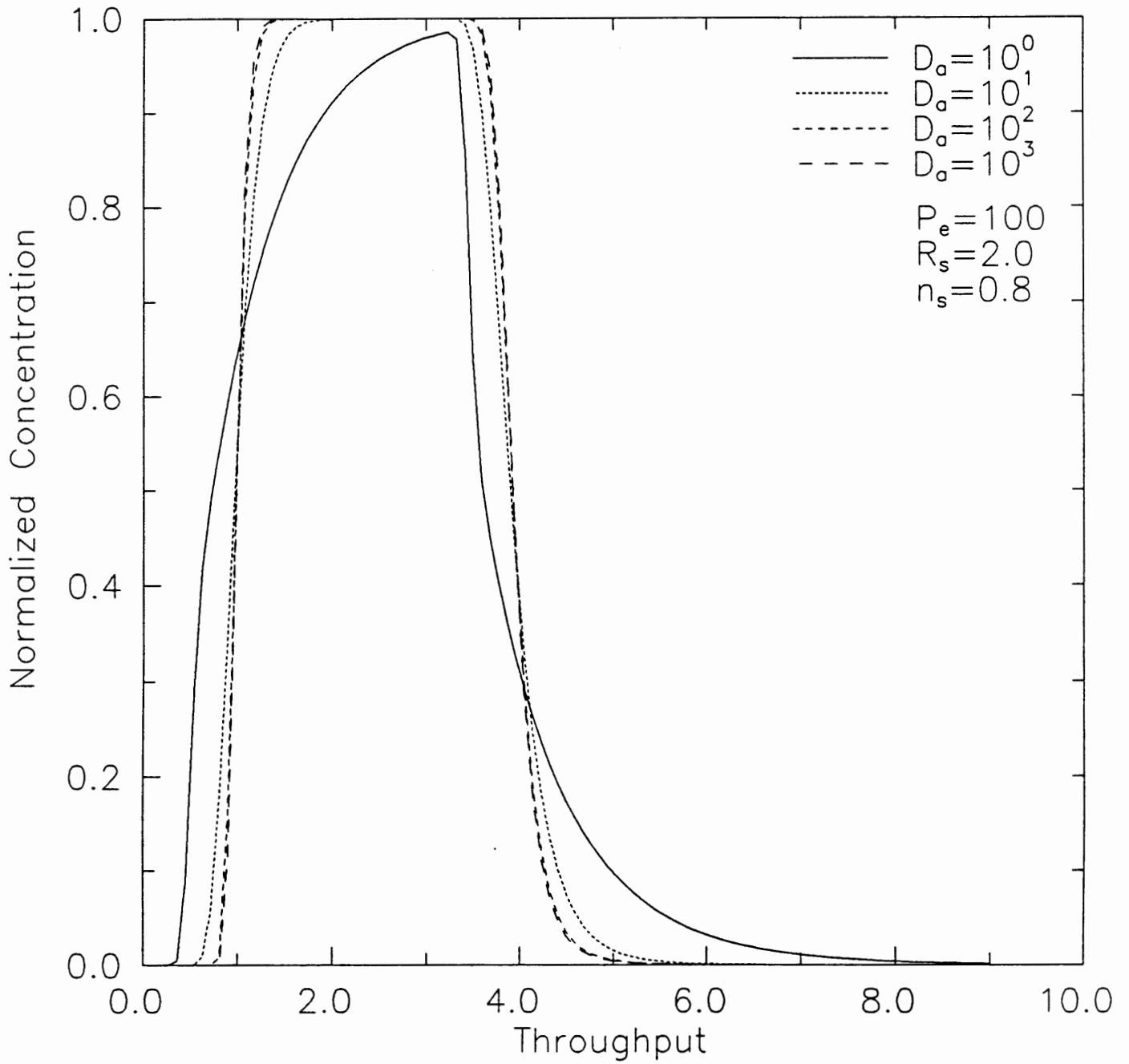


Figure 17. Normalized concentration profiles as a function of D_a for $R_f = 2.0$ and $n_f = 0.8$.

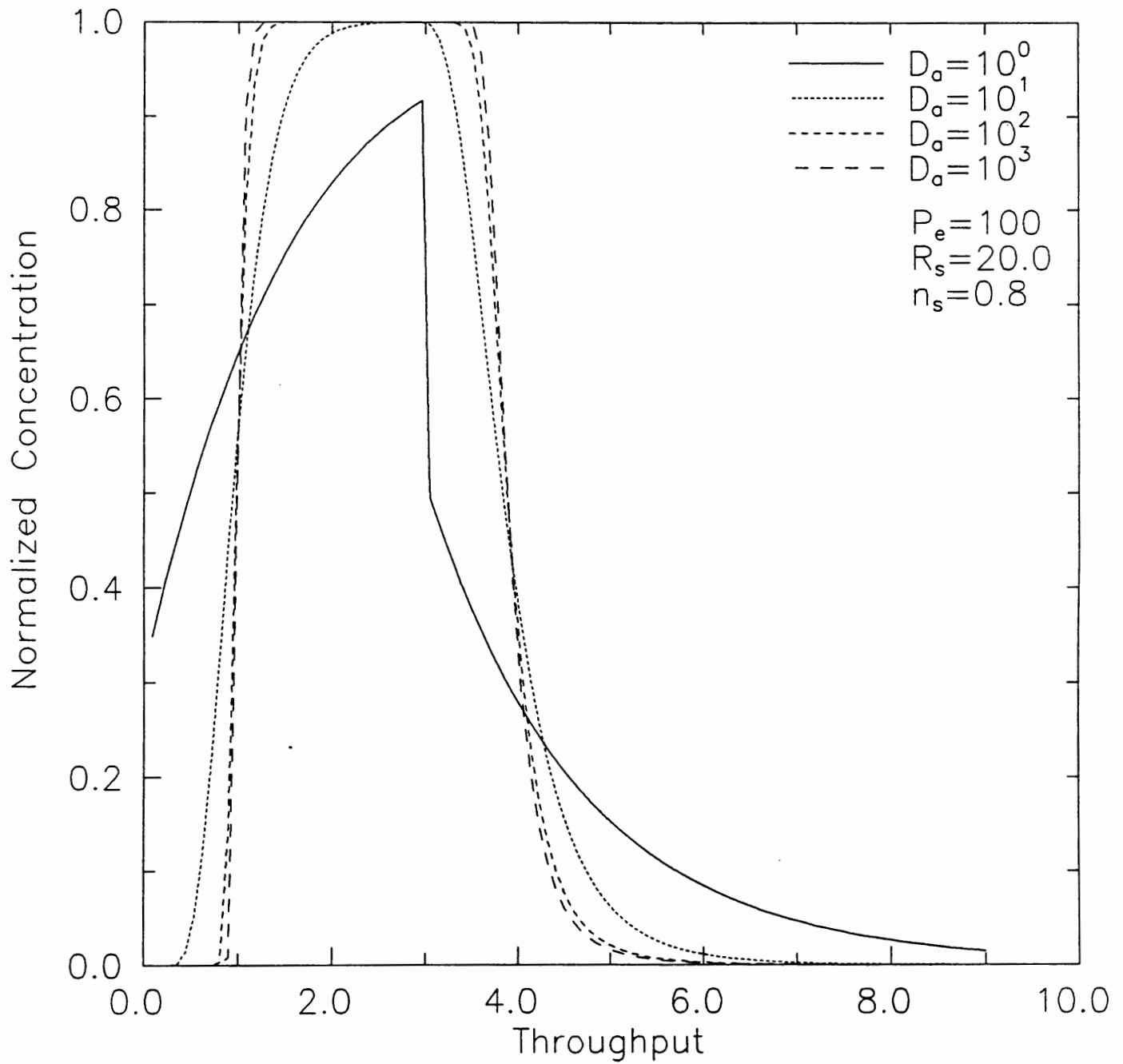


Figure 18. Normalized concentration profiles as a function of D_a for $R_f = 20.0$ and $n_f = 0.8$.

20, which show that decreasing D_a from 10 to 1 leads to roughly a doubling of the elution time for a target cleanup level of $\bar{C} = 10^{-6}$. The consistency of this result for the two values of R_f investigated suggests that this finding is consistent within the dimensionless framework presented, and it would be expected that similar results would be obtained for other values of R_f . It should be noted that different values of R_f result in varying values of \bar{t} required to meet a $\bar{C} = 10^{-6}$ cleanup level.

The general results of the rate modeling presented above can be investigated for an example case represented by results from the experimental portion of this work. A value of $\alpha = 1.22 \times 10^{-2}$ 1/hr was found for the sorption of p-dichlorobenzene to the Camp Lejeune subsurface material in laboratory studies (Table 4). Assuming this value of α is consistent with the rate of sorption and desorption in the field, conditions under which deviations from equilibrium conditions would be expected in the field can be approximated.

From Figures 19 and 20 it may be concluded that for $D_a \leq 10$ deviations from local equilibrium behavior occur and for $D_a \leq 1$ substantial deviations from local equilibrium occur. If α is assumed constant and equivalent to the laboratory-measured value of 1.22×10^{-2} 1/hr, then values of τ can be determined as a function of R_f for which deviations from local equilibrium behavior occur. The results of such an analysis give

$$\tau_c = \frac{82.0D_a}{R_f - 1} \quad (69)$$

where τ_c is the critical hydraulic retention time in hours for deviations from local equilibrium consistent with a given value of D_a to be observable.

For example to see roughly twice the required cleanup time for an aquifer as compared to local equilibrium, a D_a of 1 would be needed. For a R_f of 2 a retention time of about 82 hours would be required to see a doubling in cleanup times—very short by groundwater standards. A noticeable difference from local equilibrium conditions would occur for a hydraulic retention time of 820 hours—still short by groundwater standards.

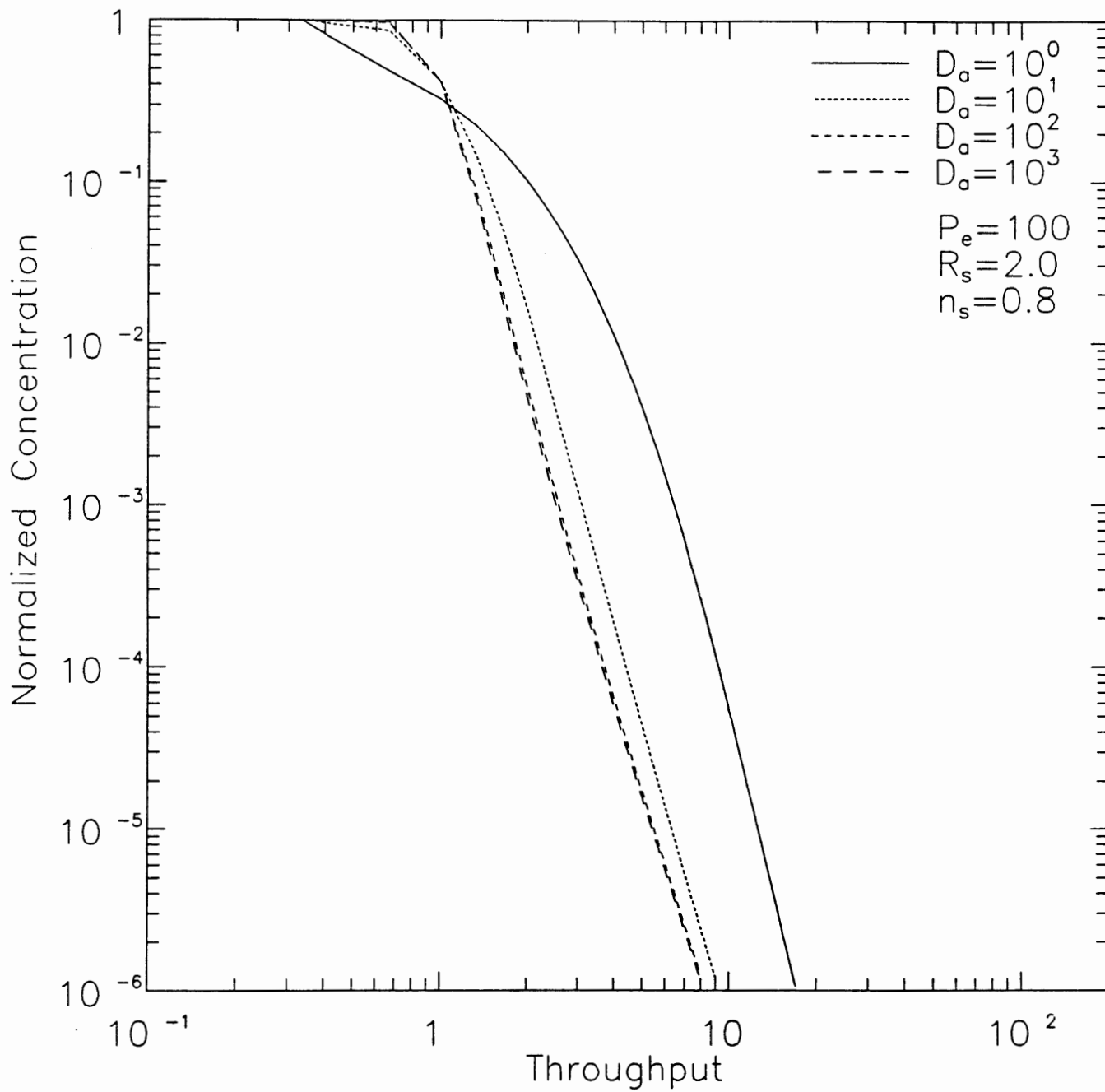


Figure 19. The effect of D_a on solute elution time required to reach low concentration action levels for $R_f = 2.0$.

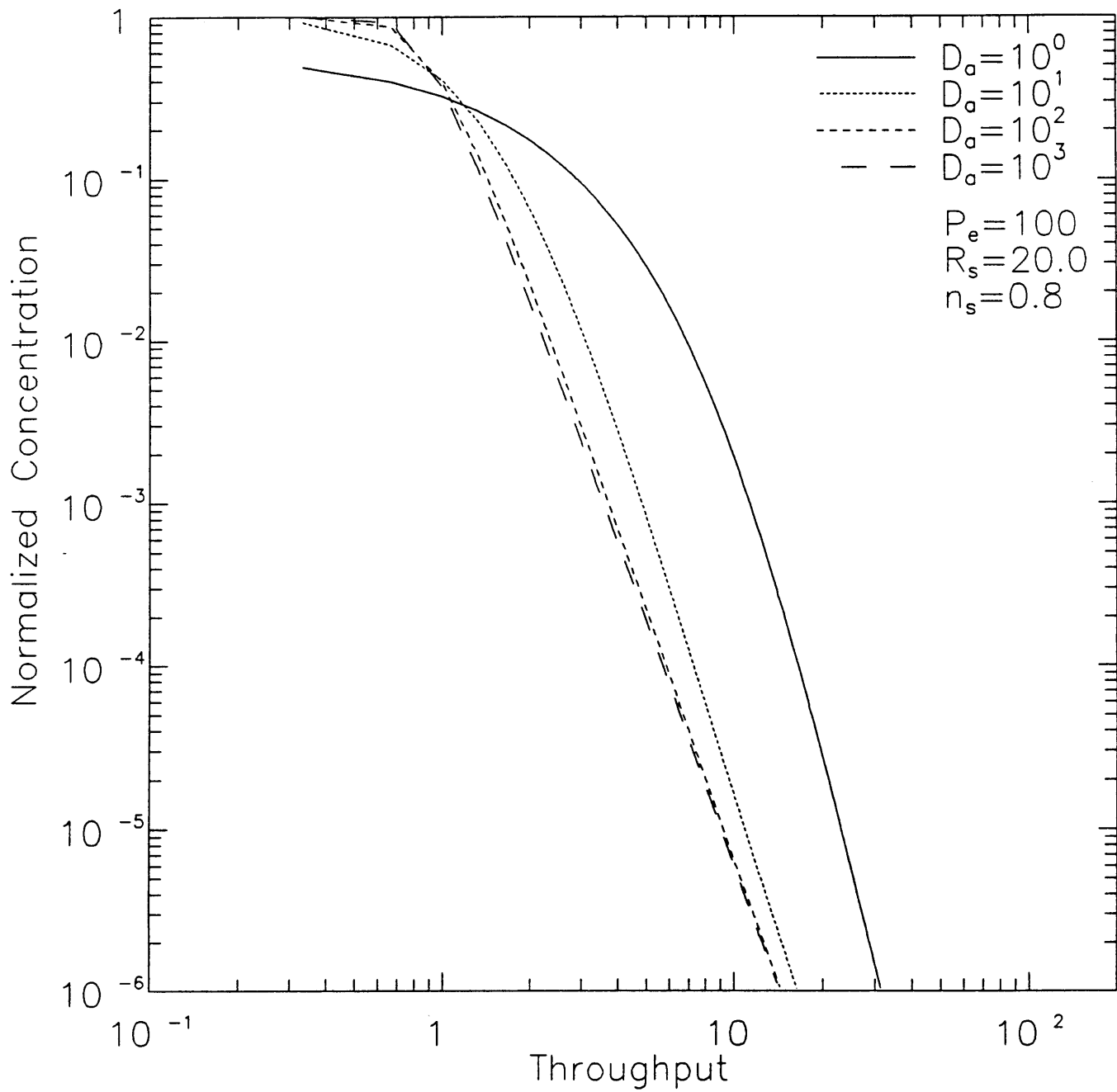


Figure 20. The effect of D_a on solute elution time required to reach low concentration action levels for $R_f = 20.0$.

Based upon the above analysis and the rates of sorption measured in the laboratory for p-dichlorobenzene and the Camp Lejeune solid material, it is concluded that sorption rate effects would be expected to play a less important role in explaining the long cleanup times observed for aquifer remediation compared to the effects of heterogeneity and nonlinear sorption equilibrium. In other words, the rate of sorption and desorption is a second-order effect contributing to long cleanup times, but it is not a primary cause of long remediation times—for solute-solid combinations that sorb at a rate similar to the systems investigated in this work.

NOTATION

[A]	coefficient matrix resulting from application of finite element spatial approximation method (dimensionless).
<i>b</i>	Langmuir isotherm sorption-energy constant (L^3M^{-1}).
{b}	vector of known boundary values resulting from application of finite element spatial approximation method ($MM^{-1}T^{-1}$).
<i>C</i>	solution-phase solute concentration (ML^{-3}).
\bar{C}	dimensionless concentration—equation 58 (dimensionless).
<i>C_e</i>	equilibrium solution-phase solute concentration (ML^{-3}).
<i>C_f</i>	final concentration in a range for computing retardation coefficient (ML^3).
\bar{C}_f	dimensionless final concentration in a range for computing retardation coefficient—equation 64 (ML^3).
<i>C_i</i>	initial concentration in a range for computing retardation coefficient (ML^3).
\bar{C}_i	initial concentration in a range for computing retardation coefficient—equation 63 (ML^3).
<i>C_o</i>	initial solution-phase solute concentration (ML^{-3}).
<i>C_s</i>	fluid-phase equilibrium-isotherm solute concentration corresponding to the solid-phase concentration at the particle boundary (ML^{-3}).
<i>D_a</i>	Damkohler number grouping of two-site model rate coefficient—equation 68 (dimensionless).
<i>D_h</i>	second-rank hydrodynamic-dispersion tensor ($L^2 T^{-1}$).
<i>D_x</i>	longitudinal hydrodynamic-dispersion coefficient in the <i>x</i> direction ($L^2 T^{-1}$).
<i>D_s</i>	intraparticle surface-diffusion coefficient for dual-resistance model (L^2T^{-1}).
<i>f_{oc}</i>	fraction of organic carbon in a solid phase (dimensionless).
<i>f_{om}</i>	fraction of organic matter in a solid phase (dimensionless).
<i>k_e</i>	effective first-order decay rate (T^{-1}).
\bar{k}_e	dimensionless effective decay rate—equation 60 (dimensionless).
<i>k_f</i>	film mass-transfer coefficient for dual-resistance model (LT^{-1}).
<i>k_{fd}</i>	first-order fluid-phase decay rate constant (T^{-1}).
<i>k_{sd}</i>	first-order solid-phase decay rate constant (T^{-1}).
<i>K_F</i>	Freundlich isotherm sorption-capacity constant ($(L^3M^{-1})^{n_F}$).
<i>K_f</i>	Freundlich isotherm sorption-capacity constant for the rapid-rate component of the two-site model ($(L^3M^{-1})^{n_f}$).
<i>K_s</i>	Freundlich isotherm sorption-capacity constant for the slow-rate component of the two-site model ($(L^3M^{-1})^{n_s}$).
<i>K_{oc}</i>	organic-carbon normalized partition coefficient (L^3M^{-1}).
<i>K_{ow}</i>	octanol:water partition coefficient (dimensionless).
<i>K_p</i>	linear sorption isotherm model coefficient (L^3M^{-1}).
<i>M</i>	mass of solid phase in batch reactor (M).
<i>M_s</i>	mass of solute initially added to batch reactor system (M).
<i>n</i>	porosity of the porous media (dimensionless).
<i>n_d</i>	number of experimental data points (dimensionless).

n_e	number of nodes in an element (dimensionless).
n_f	Freundlich isotherm sorption-energy constant for the rapid-rate component of the two-site rate model (dimensionless).
n_F	Freundlich isotherm sorption-energy constant (dimensionless).
n_n	number of nodes in a domain (dimensionless).
n_s	Freundlich isotherm sorption-energy constant for the slow-rate component of the two-site rate model (dimensionless).
N_l	Lagrange polynomial basis function—given by equation 77 (dimensionless).
P_e	Peclet number—equation 55 (dimensionless).
q	volume-average solid-phase solute mass normalized by the solid-phase mass ($M-M^{-1}$).
$\{\hat{q}'\}$	a vector of $\partial q_r / \partial t$ terms resulting from application of finite element spatial approximation method ($MM^{-1}T^{-1}$).
q_d	experimental mass-average solid-phase solute mass normalized by the solid-phase mass (MM^{-1}).
q_e	equilibrium mass-average solid-phase solute mass normalized by the solid-phase mass (MM^{-1}).
q_f	mass-average solid-phase solute mass normalized by the solid-phase mass for the rapid sorption-rate component of the two-site model (MM^{-1}).
q_{fe}	equilibrium mass-average solid-phase solute mass normalized by the solid-phase mass for the slow sorption-rate component of the two-site model (MM^{-1}).
q_m	model-predicted mass-average solid-phase solute mass normalized by the solid-phase mass (MM^{-1}).
q_o	mass-average solid-phase concentration at equilibrium corresponding to a fluid-phase concentration of C_o —equation 65 (dimensionless).
q_r	solid-phase solute mass normalized by the solid-phase mass as a function of radial position (MM^{-1}).
\hat{q}_r	trial function for solid-phase solute mass normalized by the solid-phase mass as a function of radial position (MM^{-1}).
q_s	mass-average solid-phase solute mass normalized by the solid-phase mass for the slow sorption-rate component of the two-site model (MM^{-1}).
q_{se}	equilibrium mass-average solid-phase solute mass normalized by the solid-phase mass for the slow sorption-rate component of the two-site model (MM^{-1}).
Q^o	Langmuir isotherm sorption-capacity constant (MM^{-1}).
r	radial distance variable for dual-resistance model (L).
rxn	subscript denoting a general chemical or mass-transfer reaction (dimensionless).
R	solid-phase particle radius (L).
R_{bf}	retardation factor for a batch reactor—defined by equation 11 (dimensionless).
R_f	retardation factor—defined by equation 29 (dimensionless).
srp	subscript denoting a sorption mass-transfer reaction (dimensionless).
t	time (T).
\bar{t}	throughput—equation 67 (dimensionless).
\vec{v}	average macroscopic pore-velocity vector (LT^{-1}).

v_x	pore velocity in the longitudinal direction (LT^{-1}).
V	volume of solution in a batch reactor (L^3).
W	weighting function (dimensionless).
x	longitudinal spatial location (L).
\bar{x}	dimensionless distance—equation 59 (dimensionless).
X	system length (L).
α	two-site model rate constant (T^{-1}).
$\Gamma(C)$	fluid-phase solute source ($ML^{-3}T^{-1}$).
$\Gamma(q_r)$	solid-phase solute source for the dual-resistance model ($MM^{-1} T^{-1}$).
$\Gamma(q_s)$	solid-phase solute source for the slow sites in the two-site sorption-rate model ($MM^{-1}T^{-1}$).
Δ	spatial discretization step prefix for finite difference approximation of differential equations (dimensionless).
ϵ	relative error between experimental and model data (dimensionless).
ρ	density of the solid particle (ML^{-3}).
ρ_b	bulk density of the solid phase (ML^{-3}).
τ	mean hydraulic retention time—equation 54 (T).
τ_c	critical mean hydraulic retention time for a given degree of deviation from local equilibrium—equation 69 (T).
χ	molecular connectivity index (dimensionless).

REFERENCES

- American Public Health Association. 1986. Standard Method for the Examination of Water and Wastewater, 16th Edition. American Public Health Association. American Water Works Association, and Water Pollution Control Federation.
- Anderson, M.P. 1979. Using models to simulate the movement of contaminants through groundwater flow systems. *CRC Critical Reviews in Environmental Control*. 9(2): 97-156.
- Back, W., and J.A. Cherry. 1976. Chemical aspects of present and future hydrogeological problems. In *Advances in Groundwater Hydrology*, ed. Z.A. Saleem.
- Bahr, J.M., and J. Rubin. 1987. Direct comparison of kinetic and local equilibrium formulations for solute transport affected by surface reactions. *Water Resources Research*. 23(3): 438-52.
- Bailey, G.W., and J.L. White. 1970. Factors influencing the adsorption, desorption, and movement of pesticides in soil. *Residue Review*. 32:29-92.
- Banerjee, S., S.H. Yalkowsky, and S.C. Valvani. 1980. Water solubility and octanol/water partition coefficients of organics limitations of the solubility-partition coefficient correlation. *Environmental Science & Technology*. 14(10): 1227-29.
- Bear, J. 1979. *Hydraulics of Groundwater*. New York:McGraw-Hill, Inc.
- Black, C.A. 1965. *Method of Soil Analysis—Part II*. American Society of Agronomy. Serial No. 9.
- Boucher, F.R., and G.F. Lee. 1972. Adsorption of lindane and dieldrin pesticides on unconsolidated aquifer sands. *Environmental Science & Technology*. 6(6): 538-43.
- Boyd, S.A. 1982. Adsorption of substituted phenols by soil. *Soil Science*. 134:337-43
- Browman, M.G., and G. Chesters. The solid-water interface transfer of organic pollutants across the solid-water interface. In *Fate of Pollutants in the Air and Water Environment, Part I*, ed. Suffet, I.H., New York:Wiley and Sons.
- Cameron, D.R., and A. Klute. 1977. Convective-dispersive solute transport with a combined equilibrium and kinetic adsorption model. *Water Resources Research*. 13(1): 183-88.
- Canter, L.W., and R.C. Knox. 1986. *Ground Water Pollution Control*. Chelsea, MI:Lewis Publishers.

- Chiou, C.T., P.E. Porter, and D.W. Schmedding. 1983. Partition equilibria of nonionic organic compounds between soil organic matter and water. *Environmental Science & Technology*. 17(4): 227-31.
- Chiou, C.T. 1986. Role of organic matter, minerals and moisture in sorption of nonionic compounds and pesticides by soil. In Press.
- Coates, J.T., and A.W. Elzerman. 1986. Desorption kinetics for selected PCB congeners from river sediments. *Journal of Contaminant Hydrology*. 1:191- 210.
- Crittenden, J.C., N.J. Hutzler, D.G. Geyer, J.L. Oravitz, and G. Friedman. 1986. Transport of organic compounds with saturated groundwater flow: model development and parameter sensitivity. *Water Resources Research*. 22(3): 271- 84.
- de Marsily, G. 1986. *Quantitative Hydrogeology, Groundwater Hydrology for Engineers*. Orlando, FL:Academic Press, Inc.
- DiGiano, F.A., C.T. Miller, A.C. Roche, and E.D. Wallingford. 1988. *Methodology for Assessment of Contamination of the Unsaturated Zone by Leaking Underground Storage Tanks*, Report No. 242, Water Resources Research Institute of The University of North Carolina.
- Faust, C.R., and J.W. Mercer. 1980. Ground-water modeling: recent developments. *Ground Water*. 18(6): 569-77.
- Fletcher, C.L., and D.K. Kaufman. 1980. Effect of sterilization methods on 3-chloroaniline behavior in soil. *Journal of Agricultural and Food Chemistry*. 28(3): 667-71.
- Freeze, R.A., and J.A. Cherry. 1979. *Groundwater*, Englewood Cliffs, NJ:Prentice-Hall, Inc.
- Gear, C.W. 1971. *Numerical Initial Value Problems in Ordinary Differential Equations*. Englewood Cliffs, NJ:Prentice-Hall, Inc.
- Goltz, M.N., and P.V. Roberts. 1986. Interpreting organic solute transport data from a field experiment using physical nonequilibrium models. *Journal of Contaminant Hydrology*. 1:77-93.
- Gschwend, P.M., and S. Wu. 1985. On the constancy of sediment-water partition coefficients of hydrophobic organic pollutants. *Environmental Science & Technology*. 19(1): 90-96.
- Hamaker, J.W., and J.M. Thompson. 1972. Adsorption. In *Organic Chemicals in the Soil Environment*, Vol. 1, ed. C.A.I. Goring and J.W. Hamaker, New York:Marcel Dekker, Inc.
- Hansch, C., and A.J. Leo. 1979. *Substituent Constants for Correlation Analysis in Chemistry and Biology*. New York:Wiley-Interscience.

- Hutzler, N.J., J.C. Crittenden, J.L. Oravitz, C.J. Meyer, and A.S. Johnson. 1984. Modeling groundwater transport of organic compounds. In Proc. Environ. Engr. Specialty Confer. A.S.C.E., Los Angeles, California.
- Hutzler, N.J., J.C. Crittenden, J.S. Gierke, and A.S. Johnson. 1986. Transport of organic compounds with saturated groundwater flow: experimental results. *Water Resources Research*. 22(3): 285-95.
- Huyakorn, P.S., and G.F. Pinder. 1983. *Computational Methods in Subsurface Flow*. New York:Academic Press.
- Jennings, A.A. 1987. Critical chemical reaction rates for multicomponent groundwater contamination models. *Water Resources Research*. 23(9): 1775-84.
- Kale, S.P., and K. Raghu. 1982. Efficacy of different soil sterilization methods. *Chemosphere*. 11(12): 1243-47.
- Karickhoff, S.W., D.S. Brown, and T.A. Scott. 1979. Sorption of hydrophobic pollutants on natural sediments. *Water Research*. 13:241-48.
- Karickhoff, S.W. 1980. Sorption kinetics of hydrophobic pollutants in natural sediments. In *Contaminants and Sediments, Vol. 2*, ed. R.A. Baker, Ann Arbor, MI:Ann Arbor Science Publ.
- Karickhoff, S.W. 1984. Organic pollutant sorption in aquatic systems. *Journal of Hydraulic Engineering*. 110(6): 707-35.
- Kay, B.D., and D.E. Elrick. 1967. Adsorption and movement of lindane in soils. *Soil Science*. 104(5): 314-22.
- Kenaga, E.E., and C.A.I. Goring. 1980. Relationship between water solubility, soil sorption, octanol-water partitioning, and concentrations of chemicals in biota. In *Aquatic Toxicology*, ed. J.G. Eaton, P.R. Parrish, and A. C. Hendricks.
- Leenheer, J.A., and J.L. Ahlrichs. 1971. A kinetic and equilibrium study of the adsorption of carbaryl and parathion upon soil organic matter surfaces. *Soil Sci. Soc. Amer. Proc.* 35:700-705.
- Lyman, W.J., W.F. Reehl, and D.H. Rosenblatt. 1982. *Handbook of Chemical Property Estimation Methods, Environmental Behavior of Organic Compounds*. McGraw-Hill, Inc.
- Mackay, D.M., W.P. Ball, and M.G. Durant. 1986. Variability of aquifer sorption properties in a field experiment on groundwater transport of organic solutes: methods and preliminary results. *Journal of Contaminant Hydrology*. 1:119-32.
- Means, J.C., S.G. Wood, J.J. Hassett, and W.L. Banwart. 1980. Sorption of polynuclear aromatic hydrocarbons by sediments and soils. *Environmental Science & Technology*. 14:1524-28.

- Means, J.C., S.G. Wood, J.J. Hassett, and W.L. Banwart. 1982. Sorption of carboxy-substituted polynuclear aromatic hydrocarbons by sediments and soils. *Environmental Science & Technology*. 16:93-98.
- Milanovich, F.P. 1986. Detecting chloroorganics in groundwater. *Environmental Science & Technology*. 20(5): 441-42.
- Miller, C.T. 1984. Modeling of sorption and desorption phenomena for hydrophobic organic contaminants in saturated soil environments, Ph.D. Dissertation, University of Michigan, Ann Arbor, MI.
- Miller, C.T., and W.J. Weber, Jr. 1984a. Evaluation of partitioning processes for organic contaminants in ground water. In *Proc. 2nd International Confer. on Ground Water Quality Res.*, Tulsa, Oklahoma.
- Miller, C.T., and W.J. Weber, Jr. 1984b. Modeling organic contaminant partitioning in ground water systems. *Ground Water*. 22(5): 584-92.
- Miller, C.T., and W.J. Weber, Jr. 1986. Sorption of hydrophobic compounds in saturated soil systems. *Journal of Contaminant Hydrology*. 1:243-61.
- Miller, C.T., and W.J. Weber, Jr. 1988. Modeling the sorption of hydrophobic compounds by aquifer materials—II. Column reactor studies. *Water Research*. 22(4): 465-74.
- Mingelgrin, U., and Z. Gerstl. 1983. Reevaluation of partitioning as a mechanism of non-ionic chemicals adsorption in soils. *Journal of Environmental Quality*. 12:1-11.
- Mitchell, J.K. 1976. *Fundamental of Soil Behavior*. New York:Wiley & Sons, Inc.
- Molz, F.J., O. Güven, J.G. Melville, and J.F. Keely. 1987. Performance and analysis of aquifer tracer tests with implications for contaminant transport modeling—a project summary. *Ground Water*. 25(3): 337-41.
- Morrill, L.G., B.C. Mahilum, and S.H. Mohiuddin. 1982. Organic compounds in soils: sorption, degradation, and persistence. Ann Arbor, MI:Ann Arbor Science Publ.
- Murali, V., and A.G. Aylmore. 1983. Competitive adsorption during solute transport in soils: 3. A review of experimental evidence of competitive adsorption and an evaluation of simple competition models. *Soil Science*. 135:279-89.
- Neretnieks, I. 1980. Diffusion in the rock matrix: an important factor in radionuclide retardation? *Journal of Geophysical Research*. 85(138): 4379-97.
- Parker, J.C., and A.J. Valocchi. 1986. Constraints on the validity of equilibrium and first-order kinetic transport models in structured soils. *Water Resources Research*. 22(3): 399-407.

- Pedit, J.A., and C.T. Miller. 1988. The advantage of high-order basis functions for modeling multicomponent sorption kinetics. In *International Conference on Computational Methods in Water Resources (7th, Cambridge, Massachusetts)*, Computational Methods in Water Resources, Vol. 2 Numerical Methods for Transport and Hydrologic Processes, ed. M.A. Celia, L.A. Ferrand, C.A. Brebbia, W.G. Gray, and G.F. Pinder, Southampton, U.K.:Computational Mechanics Publications.
- Pierce, R.H., Jr., C.E. Olney, and G.T. Felbeck, Jr. 1971. Pesticide adsorption in soils and sediments. *Environmental Letters*. 1(2): 157-72.
- Prickett, T.A., T.C. Naymik, and C.G. Lonnquist. 1981. A "random walk" solute transport model for selected groundwater quality evaluations, *Illinois Water Survey Bulletin* 65.
- Rasmuson, A. 1981. Exact solution of a model for diffusion and transient adsorption in particles and longitudinal dispersion in packed beds. *Amer. Inst. of Chem. Eng. Journal*. 27(6): 1032-35.
- Rasmuson, A., and I. Neretnieks. 1980. Exact solution of a model for diffusion in particles and longitudinal dispersion in packed beds. *Amer. Inst. of Chem. Eng. Journal*. 26(4): 686-89.
- Rasmuson, A., T.N. Narasimhan, and I. Neretnieks. 1982. Chemical transport in fissured rock: verification of a numerical model. *Water Resources Research*. 18(5): 1479-92.
- Roberts, P.V., M. Reinhard, and A.J. Valocchi. 1982. Movement of organic contaminants in ground water: implications for water supply. *Journal AWWA*. 74(8): 408-13.
- Sabljić, A. 1987. On the prediction of soil sorption coefficients of organic pollutants from molecular structure: application of molecular topology model. *Environmental Science & Technology*. 21:358-66.
- Selim, H.M., J.M. Davidson, and R.S. Mansell. 1976. Evaluation of a two-site adsorption-desorption model for describing solute transport in soils. In *Proc. Summer Computer Simulation Conf.*, Washington, D.C.
- Stauffer, T.B., and W.G. MacIntyre. 1986. Sorption of low-polarity organic compounds on oxide minerals and aquifer material. *Environmental Toxicology and Chemistry*. 5(11): 949-55.
- Sudicky, E.A. 1986. A natural gradient experiment on solute transport in a sand aquifer: spatial variability of hydraulic conductivity and its role in the dispersion process. *Water Resource Research*. 22(13): 2069-82.
- Swanson, R.A., and G.R. Dutt. 1973. Chemical and physical processes that affect atrazine and distribution in soil systems. *Soil Science Society of America Proceedings*. 37:872-76.

- Valocchi, A.J. 1985. Validity of the local equilibrium assumption for modeling sorbing solute transport through homogeneous soils. *Water Resources Research*. 21(6): 808–20.
- Valocchi, A.J. 1986. Effect of radial flow on deviations from local equilibrium during sorbing solute transport through homogeneous soils. *Water Resources Research*. 22(12): 1693–1701.
- Van Genuchten, M.T., and P.J. Wierenga. 1976. Mass transfer studies in sorbing porous media I. Analytical Solutions. *Soil Science Society of America Journal*. 40(4): 473–80.
- Van Genuchten, M.T., and P.J. Wierenga. 1977. Mass transfer studies in sorbing porous media: II. Experimental evaluation with tritium ($^3\text{H}_2\text{O}$). *Soil Science Society of America Journal*. 41:272–78.
- Van Genuchten, M.T., P.J. Wierenga, and G.A. O'Connor. 1977. Mass transfer studies in sorbing porous media: III. Experimental evaluation with 2,4,5-T. *Soil Science Society of America Journal*. 41:278–85.
- Verschueren, K. 1983. *Handbook of Environmental Data on Organic Chemicals*. New York: Van Nostrand Reinhold Company.
- Voice, T.C., and W.J. Weber, Jr. 1983. Sorption of hydrophobic compounds by sediments, soils and suspended solids—I: theory and background. *Water Research*. 17(10): 1433–41.
- Weber, W.J., L.E. Katz, B.E. Jacobs, and C.T. Miller. 1986. Competitive sorption reactions in subsurface systems. Presented at: American Geophysical Union Fall Meeting Paper No. H31A-09 1130H.
- Weber, W.J., Jr., and C.T. Miller. 1988. Modeling the sorption of hydrophobic compounds by aquifer materials—I. Rates and equilibria. *Water Research*. 22(4): 457–64.
- Weber, J.B., and C.T. Miller. 1989. Movement of organic chemicals over and through soil. In *Reactions and Movement of Organic Chemicals in Soils*, ed. B.L. Sawhney, Madison, WI: Soil Science Society of America, Inc.
- Woodburn, K.B., P.S.C. Rao, M. Fukui, and P. Nkedi-Kizza. 1986. Solvophobic approach for predicting sorption of hydrophobic organic chemicals on synthetic sorbents and soils. *Journal of Contaminant Hydrology*. 1:227–41.
- Wu, S., and P.M. Gschwend. 1986. Sorption kinetics of hydrophobic organic compounds to natural sediments and soils. *Environmental Science & Technology*. 20(7): 717–25.

**APPENDIX I. FINITE ELEMENT DERIVATION FOR
DUAL-RESISTANCE BATCH MODEL**

Consider the dual-resistance model for a batch reactor given by the fluid-phase equation,

$$\frac{dC}{dt} = -\frac{3k_f M}{RV\rho}(C - C_s) - k_{fd}C \quad (70)$$

the solid-phase equation,

$$\frac{\partial q_r}{\partial t} = \frac{D_s}{r^2} \frac{\partial}{\partial r} \left(r^2 \frac{\partial q_r}{\partial r} \right) - k_{sd}q_r \quad (71)$$

the solid-phase boundary conditions,

$$\left. \frac{\partial q_r}{\partial r} \right|_{r=R} = \frac{k_f}{D_s \rho} (C - C_s) \quad (72)$$

$$\left. \frac{\partial q_r}{\partial r} \right|_{r=0} = 0 \quad (73)$$

and the initial conditions

$$C(t = 0) = C_0 \quad (74)$$

$$q_r(0 \leq r \leq R, t = 0) = 0 \quad (75)$$

The Galerkin finite element method may be used to approximate the spatial derivative in Equation 71 by first defining a trial function

$$\hat{q}_r(r) = \sum_{l=1}^{n_n} N_l(r)q_{rl} \quad (76)$$

where N_l are the Lagrange polynomial basis functions given by

$$N_l(r) = \prod_{\substack{L=1 \\ L \neq l}}^{n_e} \frac{r - r_L}{r_l - r_L} \quad (77)$$

where: l is a node index; r_l and r_L are the locations of node l and node L ; n_n is the total number of nodes; and n_e is the number of nodes in an element. The number of nodes in an element determines the order of the Lagrange polynomial basis function. Seven nodes per element were used to yield sixth-order elements.

The weighted residual method requires that a system of equations—one equation for each node in the discretized domain—when formed with respect to the governing partial differential equation and integrated over the domain vanish, which gives for the solid-phase equation

$$\int_0^R W_k \left[\frac{D_s}{r^2} \frac{\partial}{\partial r} \left(r^2 \frac{\partial \hat{q}_r}{\partial r} \right) - k_{sd} \hat{q}_r - \frac{\partial \hat{q}_r}{\partial t} \right] r^2 dr = 0 \quad (78)$$

for $k = 1, \dots, n_n$

where W_k is a weighting function. The Galerkin finite element method requires that the weighting function be equivalent to the basis function, which gives

$$\int_0^R N_k \left[\frac{D_s}{r^2} \frac{\partial}{\partial r} \left(r^2 \frac{\partial \hat{q}_r}{\partial r} \right) - k_{sd} \hat{q}_r - \frac{\partial \hat{q}_r}{\partial t} \right] r^2 dr = 0 \quad (79)$$

for $k = 1, \dots, n_n$

Accuracy and stability of the Galerkin finite element require that the requirements of completeness and consistency be met (Huyakorn and Pinder, 1983). Thus, since the Lagrange polynomials are C^0 continuous—interpolation of the dependent variable is continuous at element boundaries, but interpolation of any derivative of the dependent variable is not continuous, it is necessary to reduce the second-order partial derivative in Equation 79 by integrating by parts

$$\int_0^R N_k \frac{\partial \hat{q}_r}{\partial t} r^2 dr = -D_s \int_0^R \frac{dN_k}{dr} \frac{\partial \hat{q}_r}{\partial r} r^2 dr - \int_0^R k_{sd} N_k \hat{q}_r r^2 dr + D_s N_k r^2 \frac{\partial \hat{q}_r}{\partial r} \Big|_{r=0}^{r=R} \quad (80)$$

for $k = 1, \dots, n_n$

which may be written in matrix-vector notation as

$$[\mathbf{A}]\{\hat{\mathbf{q}}'\} = \{\mathbf{b}\} \quad (81)$$

where; $[\mathbf{A}]$ is a coefficient matrix resulting from solution of the left-hand-side of Equation 81; $\{\hat{\mathbf{q}}'\}$ is vector of dq_r/dt terms corresponding to each radial node; and $\{\mathbf{b}\}$ is a vector resulting from evaluation of the right-hand-side of Equation 81 for a given vector $\{\hat{\mathbf{q}}_r\}$.

Equation 81 was combined with Equation 71, subject to the boundary and initial conditions—yielding a system of $n_n + 1$ ordinary differential equations in time. The system of equations was solved using Gear's method for stiff equations (Gear, 1971).

**APPENDIX II. FINITE DIFFERENCE DERIVATION FOR
ONE-DIMENSIONAL TWO-SITE MODEL**

Consider the ADR form of a two-site sorption model given by the fluid-phase equation,

$$R_f \frac{\partial C}{\partial t} = D_x \frac{\partial^2 C}{\partial x^2} - v_x \frac{\partial C}{\partial x} - \frac{\rho_b}{n} [k_{sd} K_f C^{n_f} + \alpha (K_s C^{n_s} - q_s)] - k_{fd} C \quad (82)$$

the solid-phase equation,

$$\frac{dq_s}{dt} = \alpha (K_s C^{n_s} - q_s) - k_{sd} q_s \quad (83)$$

the boundary conditions,

$$C(t > 0, x = 0) = C_0 \quad (84)$$

$$\left. \frac{\partial C}{\partial x} \right|_X = 0 \quad (85)$$

and the initial conditions

$$C(t = 0, x) = 0 \quad (86)$$

$$q_s(t = 0, x) = 0 \quad (87)$$

where

$$R_f = 1 + \frac{\rho_b}{n} n_f K_f C^{n_f - 1} \quad (88)$$

The finite-difference approximation for equation 82 is

$$R_{f,i} \frac{dC_i}{dt} = D_x \left(\frac{C_{i-1} + C_{i+1} - 2C_i}{\Delta x^2} \right) - v_x \left(\frac{C_{i+1} - C_{i-1}}{2\Delta x} \right) - k_{fd} C_i - \frac{\rho_b}{n} [k_{sd} K_f C_i^{n_f} + \alpha (K_s C_i^{n_s} - q_s)] \quad (89)$$

for the Freundlich sorption-equilibrium-based retardation coefficient defined as

$$R_{f,i} = 1 + \frac{n_f K_f \rho_b}{n} C_i^{n_f - 1} \quad (90)$$

where i is a spatial node index.

Equation 89 can be rearranged to give

$$\begin{aligned} \frac{dC_i}{dt} = & \frac{1}{R_{f,i}} \left(\frac{D_x}{\Delta x^2} + \frac{v_x}{2\Delta x} \right) C_{i-1} + \frac{1}{R_{f,i}} \left(-\frac{2D_x}{\Delta x^2} - k_{fd} \right) C_i + \frac{1}{R_{f,i}} \left(\frac{D_x}{\Delta x^2} - \frac{v_x}{2\Delta x} \right) C_{i+1} \\ & - \frac{\rho_b}{R_{f,i} n} [k_{sd} K_f C_i^{n_f} + \alpha (K_f C_i^{n_s} - q_s)] \end{aligned} \quad (91)$$

The solid-phase equation for the slow component at the i th node is

$$\frac{dq_{s,i}}{dt} = \alpha (K_s C_i^{n_s} - q_{s,i}) - k_{sd} q_{s,i} \quad (92)$$

For sharp-front problems that result from a small dispersion coefficient, Equation 91 formally changes type from parabolic to hyperbolic. The hyperbolic-form of the ADR equation is notoriously difficult to solve accurately (Huyakorn and Pinder, 1983). A review of the methods used to approximate the hyperbolic form of the ADR equation is beyond the scope of this report. The upwind method is frequently used for finite difference approximations for hyperbolic problems and is given by

$$\begin{aligned} \frac{dC_i}{dt} = & \frac{1}{R_{f,i}} \left(\frac{D_x}{\Delta x^2} + \frac{v_x}{\Delta x} \right) C_{i-1} + \frac{1}{R_{f,i}} \left(-\frac{2D_x}{\Delta x^2} - \frac{v_x}{\Delta x} - k_{fd} \right) C_i + \frac{1}{R_{f,i}} \left(\frac{D_x}{\Delta x^2} \right) C_{i+1} \\ & - \frac{\rho_b}{R_{f,i} n} [k_{sd} K_f C_i^{n_f} + \alpha (K_f C_i^{n_s} - q_s)] \end{aligned} \quad (93)$$

which yields a spatially first-order correct solution that is more smeared in space but has less overshoot of the actual maximum concentration (Huyakorn and Pinder, 1983).

The system of ordinary differential equations resulting from the finite difference approximation to the fluid-phase equation—Equation 91 or Equation 93—and the solid-phase equation (Equation 92) were assembled and solved with respect to the boundary and initial conditions using Gear's algorithm for stiff equations (Gear, 1971).

**APPENDIX III. FINITE DIFFERENCE DERIVATION FOR
ONE-DIMENSIONAL DUAL-RESISTANCE MODEL**

Consider the ADR form of a dual-resistance sorption model given by the fluid-phase equation,

$$\frac{\partial C}{\partial t} = D_x \frac{\partial^2 C}{\partial x^2} - v_x \frac{\partial C}{\partial x} - \frac{3(1-n)k_f}{nR} (C - C_s) - k_{fd}C \quad (94)$$

the solid-phase equation,

$$\frac{\partial q_r}{\partial t} = \frac{D_s}{r^2} \frac{\partial}{\partial r} \left(r^2 \frac{\partial q_r}{\partial r} \right) - k_{sd}q_r \quad (95)$$

the fluid and solid phase-coupling equation,

$$C_s = \left(\frac{q_r}{K_F} \right)^{\frac{1}{n_F}} \quad \text{at } r = R \quad (96)$$

the boundary conditions,

$$\left. \frac{\partial q_r}{\partial r} \right|_{r=R} = \frac{k_f}{D_s \rho} (C - C_s) \quad (97)$$

$$\left. \frac{\partial q_r}{\partial r} \right|_{r=0} = 0 \quad (98)$$

and the initial conditions

$$C(t, x = 0) = C_0 \quad (99)$$

The finite-difference solution for the case of constant spatial discretization, hydrodynamic dispersion, and velocity is

$$\frac{dC}{dt} = D_x \left(\frac{C_{i-1} + C_{i+1} - 2C_i}{\Delta x^2} \right) - v_x \left(\frac{C_{i+1} - C_{i-1}}{2\Delta x} \right) - \frac{3k_f(1-n)}{Rn} (C_i - C_{s,i}) - k_{fd}C_i \quad (100)$$

where i is a spatial nodal index.

Collecting all terms involving C_{i-1} , C_i , and C_{i+1} gives

$$\begin{aligned} \frac{dC}{dt} = & \left(\frac{D_h}{\Delta x^2} + \frac{v_x}{2\Delta x} \right) C_{i-1} - \left(\frac{2D_h}{\Delta x^2} + \frac{3k_f(1-n)}{Rn} + k_{fd} \right) C_i \\ & + \left(\frac{D_h}{\Delta x^2} - \frac{v_x}{2\Delta x} \right) C_{i+1} + \left(\frac{3k_f(1-n)}{Rn} \right) C_{s,i} \end{aligned} \quad (101)$$

at the exit point

$$\begin{aligned} \left. \frac{dC}{dt} \right|_{x=X} = & \left[\left(\frac{D_h}{\Delta x^2} + \frac{v_x}{2\Delta x} \right) + \left(\frac{D_h}{\Delta x^2} - \frac{v_x}{2\Delta x} \right) \right] C_{i-1} \\ & - \left(\frac{2D_h}{\Delta x^2} + \frac{3k_f(1-n)}{Rn} + k_{fd} \right) C_i + \left(\frac{3k_f(1-n)}{Rn} \right) C_{s,i} \end{aligned} \quad (102)$$

The solid-phase equations must be solved simultaneously with the fluid-phase equations. The finite difference approximation for the solid-phase equation is

$$\frac{dq_r}{dt} = D_s \left(\frac{q_{r,l+1} - q_{r,l}}{\Delta r \Delta r_+} \right) - D_s \left(\frac{q_{r,l} - q_{r,l-1}}{\Delta r \Delta r_-} \right) + D_s \left(\frac{q_{r,l+1} - q_{r,l-1}}{r \Delta r} \right) - k_{sd} q_{r,l} \quad (103)$$

where

$$\Delta r = \frac{r_{l+1} - r_{l-1}}{2} = \frac{\Delta r_+ + \Delta r_-}{2} \quad (104)$$

$$\Delta r_- = \frac{r_l - r_{l-1}}{2} \quad (105)$$

$$\Delta r_+ = \frac{r_{l+1} - r_l}{2} \quad (106)$$

Collecting like terms involving $q_{r,l+1}$, $q_{r,l}$, and $q_{r,l-1}$ yields

$$\begin{aligned} \frac{dq_r}{dt} = & \left(\frac{D_s}{\Delta r \Delta r_-} - \frac{D_s}{r \Delta r} \right) q_{r,l-1} + \left(-\frac{D_s}{\Delta r \Delta r_-} - \frac{D_s}{\Delta r \Delta r_+} - k_{sd} \right) q_{r,l} \\ & + \left(\frac{D_s}{\Delta r \Delta r_+} + \frac{D_s}{r \Delta r} \right) q_{r,l+1} \end{aligned} \quad (107)$$

for the exterior boundary condition of the particle

$$\left. \frac{\partial q}{\partial r} \right|_R = \frac{k_f}{D_s \rho} (C - C_s) \quad (108)$$

introducing an artificial node to approximate the boundary condition yields

$$\left. \frac{q_{r,l+1} - q_{r,l-1}}{2\Delta r} \right|_R = \frac{k_f}{D_s \rho} (C - C_s) \quad (109)$$

Solving for the artificial node gives

$$q_{r,l+1} = q_{r,l-1} + \frac{2k_f \Delta r}{D_s \rho} (C - C_s) \quad (110)$$

which can be substituted into Equation 107 at the exterior of the particle to form the flux boundary condition.

The interior boundary condition poses some additional difficulty because the radial location, r , vanishes, which is an entry in the denominator of the finite difference approximation to the first spatial derivative term.

$$\frac{\partial q_r}{\partial t} = D_s \frac{\partial^2 q_r}{\partial r^2} + \frac{2D_s}{r} \frac{\partial q_r}{\partial r} - k_{sd} q_r \quad (111)$$

Recall l'Hôpital's rule

$$\lim_{r \rightarrow a} \frac{h(r)}{g(r)} = \lim_{r \rightarrow a} \frac{h'(r)}{g'(r)} \quad (112)$$

if

$$g(0) = 0 \quad (113)$$

$$h(0) = 0 \quad (114)$$

$$g'(r \neq 0) \neq 0 \quad (115)$$

For the radial diffusion problem define the functions

$$h(r) = \frac{\partial q_r}{\partial r} \quad (116)$$

$$g(r) = \frac{r}{2D_s} \quad (117)$$

then

$$\frac{h(r)}{g(r)} = \frac{2D_s}{r} \frac{\partial q_r}{\partial r} \quad (118)$$

therefore applying l'Hôpital's rule at $r = 0$ gives

$$\lim_{r \rightarrow 0} \frac{h'(r)}{g'(r)} = \lim_{r \rightarrow 0} 2D_s \frac{\partial^2 q_r}{\partial r^2} \quad (119)$$

which may be combined with Equation 111 to give

$$\left. \frac{\partial q_r}{\partial t} \right|_{r=0} = 3D_s \frac{\partial^2 q_r}{\partial r^2} - k_{sd} q_r \quad (120)$$

Approximating Equation 120 by using an artificial node $q_{r,l-1}$ gives

$$\left. \frac{\partial q_r}{\partial t} \right|_{r=0} = 3 \left[D_{s+} \left(\frac{q_{r,l+1} - q_{r,l}}{\Delta r \Delta r_+} \right) - D_{s-} \left(\frac{q_{r,l} - q_{r,l-1}}{\Delta r \Delta r_-} \right) \right] - k_{sd} q_r \quad (121)$$

Since the spatial derivative is zero at the center of the particle then the following may be applied

$$q_{r,l-1} = q_{r,l+1} \quad (122)$$

$$\Delta r_- = \Delta r_+ = \Delta r \quad (123)$$

Combining Equations 121 to 123 gives

$$\left. \frac{\partial q_r}{\partial t} \right|_{r=0} = 6D_s \left(\frac{q_{r,l+1} - q_{r,l}}{\Delta r^2} \right) - k_{sd} q_r \quad (124)$$

The above finite difference approximations result in a system of ordinary differential equations that were solved simultaneously using Gear's method for stiff equations (1971). Note that the hyperbolic form of the ADR equation can be solved in upwind form, similar to that presented in Appendix II, to reduce the well-known overshoot and oscillation problems associated with the finite difference method—at the expense of increasing numerical dispersion.